Theses and Dissertations   1. Thesis and Dissertation Collection, all items

1986

Broadband techniques applied to shipboard HF slot antennas

Neiva, Mario Cabral.

Monterey, California: U.S. Naval Postgraduate School

http://hdl.handle.net/10945/21696

NPS-62-86-005

NAVAL POSTGRADUATE SCHOOL
Monterey, California

THESIS

BROADBAND TECHNIQUES
APPLIED TO
SHIPBOARD HF SLOT ANTENNAS

by

Mário Cabral Neiva

June 1986

Thesis Advisor :   Richard W. Adler

Approved for public release; distribution is unlimited

T232201

NAVAL POSTGRADUATE SCHOOL
Monterey, CA 93943

Rear Admiral R. H. Shumaker   D. A. Schrady
Superintendent   Provost

                         Released by:

REPORT DOCUMENTATION PAGE

1a. REPORT SECURITY CLASSIFICATION UNCLASSIFIED		1b. RESTRICTIVE MARKINGS		
2a. SECURITY CLASSIFICATION AUTHORITY		3. DISTRIBUTION / AVAILABILITY OF REPORT Approved for public release; distribution is unlimited		
2b. DECLASSIFICATION / DOWNGRADING SCHEDULE				
4. PERFORMING ORGANIZATION REPORT NUMBER(S) NPS-62-86-005		5. MONITORING ORGANIZATION REPORT NUMBER(S)		
6a. NAME OF PERFORMING ORGANIZATION Naval Postgraduate School	6b. OFFICE SYMBOL (If applicable) Code 62	7a. NAME OF MONITORING ORGANIZATION Naval Ocean Systems Center		
6c. ADDRESS (City, State, and ZIP Code) Monterey, California 93943-5000		7b. ADDRESS (City, State, and ZIP Code) San Diego, California 92152		
8a. NAME OF FUNDING / SPONSORING ORGANIZATION Naval Ocean Systems Center	8b. OFFICE SYMBOL (If applicable) Code 825	9. PROCUREMENT INSTRUMENT IDENTIFICATION NUMBER		

8c. ADDRESS (City, State, and ZIP Code) San Diego, California 92152	10. SOURCE OF FUNDING NUMBERS			
	PROGRAM ELEMENT NO.	PROJECT NO.	TASK NO.	WORK UNIT ACCESSION NO.

11. TITLE (Include Security Classification)

BROADBAND TECHNIQUES APPLIED TO SHIPBOARD HF SLOT ANTENNAS

12. PERSONAL AUTHOR(S)
Neiva, Mário C.

13a. TYPE OF REPORT Master's Thesis	13b. TIME COVERED FROM _____ TO _____	14. DATE OF REPORT (Year, Month, Day) 1986, June	15 PAGE COUNT 75

16. SUPPLEMENTARY NOTATION

17	COSATI CODES		18. SUBJECT TERMS (Continue on reverse if necessary and identify by block number)
FIELD	GROUP	SUB-GROUP	Combat Survivable Antenna; Computer Modeling of Antennas

19 ABSTRACT (Continue on reverse if necessary and identify by block number)

One of the major problems in communications aboard ships is the minimization of the number of antennas, avoiding undesirable coupling between them and interference between links, therefore reducing the exposed area of ships.

In the future, for the next generation of ships the trend will be the elimination of tall and large structures to make antennas more survivable during combat.

The use of slot antennas along the bulkheads of the superstructure and broadband techniques applied to them seems to be a good candidate for solving these problems.

This thesis investigates a model of a slot antenna using the Numerical Electromagnetics Code(NEC). Input impedance, near field inside the slot and radiation patterns are presented.

20 DISTRIBUTION / AVAILABILITY OF ABSTRACT ☒ UNCLASSIFIED/UNLIMITED ☐ SAME AS RPT. ☐ DTIC USERS	21. ABSTRACT SECURITY CLASSIFICATION Unclassified	
22a. NAME OF RESPONSIBLE INDIVIDUAL Prof. Richard W. Adler	22b. TELEPHONE (Include Area Code) (408) 646-2352	22c. OFFICE SYMBOL Code 62Ab

DD FORM 1473, 84 MAR   83 APR edition may be used until exhausted   SECURITY CLASSIFICATION OF THIS PAGE
All other editions are obsolete

UNCLASSIFIED

BROADBAND TECHNIQUES
APPLIED TO
SHIPBOARD HF SLOT ANTENNAS

by

Mario Cabral Neiva
LCDR, BRAZILIAN NAVY
B.S., BRAZILIAN NAVAL ACADEMY, 1969
B.S.E.E., UNIVERSITY OF SAO PAULO, 1975

Submitted in partial fulfillment of the
requirements for the degree of

MASTER OF SCIENCE IN ELECTRICAL ENGINEERING

from the

NAVAL POSTGRADUATE SCHOOL
June 1986

ABSTRACT

One of the major problems in communications aboard ships is the minimization of the number of antennas, avoiding undesirable coupling between them and interference between links, therefore reducing the exposed area of ships.

In the future, for the next generation of ships the trend will be the elimination of tall and large structures to make antennas more survivable during combat.

The use of slot antennas along the bulkheads of the superstructure and broadband techniques applied to them seems to be a good candidate for solving these problems.

This thesis investigates a model of a slot antenna using the Numerical Electromagnetics Code (NEC). Input impedance, near field inside the slot and radiation patterns are presented .

TABLE OF CONTENTS

LIST OF TABLES

LIST OF FIGURES

ACKNOWLEDGEMENTS

I am indebted to those who have contributed their encouragement, assistance, and patience before and during the preparation of this thesis.

First to Dr. Richard W. Adler, my thesis advisor, I want to express my thanks for his patient and unfailing guidance throughout this work.

To almost 150,000,000 Brazilian tax-payers, I express my sincere appreciation for having provided funds for my course.

To Prof. Hung-Mou Lee, the second reader, my thanks for the notes and comments he made.

I owe a debt of gratitude to my parents, Emilia and Adelmy, for the intellectual background they both helped me to build since my very early years.

Finally, I would like to thank my wife, Nelma, for her continuing support, understanding, and patient help throughout NPS.

I. INTRODUCTION

A. SCOPE OF THE STUDY

One of the major problems in communications aboard ships is the minimization of the number of antennas, avoiding undesirable coupling between them and interference between links.

In the areas of antenna and propagation, however, major advances in performance have not been easily achieved. This is due mainly to the non-deterministic behavior of ionosphere and because of antennas size limitations imposed by survivability and/or visibility profile requirements. It should not be forgotten that electrically small antennas have narrow bandwidth, strong platform interaction and undesirable coupling to cosited antennas.

In the last years, the decks and superstructures aboard naval ships have become much too cluttered with antennas of all types and sizes. It can be said that, in general, one antenna was installed for each HF transmitter, transceiver, or receiver.

Major advances in communication equipment performance and size reduction have been achieved because of solid state technology. But efficient antennas have to be on the order of a quarter wavelength in size and antenna miniaturization is not easily achieved at the longer wavelengths. (At a frequency of 2 MHz, a quarter wavelength vertical antenna would have to be 37.5 meters high. Such antenna might be seen as "elctrically small" but not small physically).

Mutual coupling of cosited antennas can deteriorate the performance of communication systems involving a number of radios operating on adjacent frequencies. The situation occurs in shipborne platforms where simultaneous transmission and reception takes place. Crosstalk

interference due to mutual coupling of cosited antennas is often very difficult to mitigate in such installations.

The elimination of tall and large structures will make antennas more survivable during combat.

In the future, for the next generation of ships, the trend will be to build ships without masts, using their bulkheads along the superstructure to deploy, for example, slot antennas which seems to be good candidates for solving these problems.

This paper is an investigation of the performance of an HF slot deployed on a simulated bulkhead, created by a wire-grid wall, using a special computer program called NEC-Numerical Electromagnetics Code. (A brief description of NEC is given in Chapter III).

The understanding of linear antennas has been advanced since the late 1960's by the introduction of the METHOD OF MOMENTS. Versatile computer codes based on this method, like NEC, allow very complex antenna systems to be analyzed.

In Chapter V results for input impedance, radiation pattern, and bandwidth of the slot antennas are shown. An attempt to find the best way to feed the slots using the standard transmission lines is another goal of this thesis.

B. REVIEW OF PAST WORKS

In 1954, A. Young studied [Ref. 1] how to solve integral equations using approximate product-integration, without the aid of a digital computer.

K.K.Mei published a paper [Ref. 2] in 1965 describing the use of Hallen's integral equation for thin wire antennas, during a time when large digital computers were emerging.

To solve scattering problems using Pocklington's integral equation , one procedure is to reduce the integral equation to a system of simultaneous linear equations. R. F. Harrington in 1967 used the Method of Moments [Ref. 3] for

treating field problems. He described the use of pulse and piecewise linear current basis functions to solve the scalar and vector potential functions.

In 1950, N. Begovich studied the resonant slot antenna in an infinite plane conductor [Ref. 4].

In 1978, G. J. Burke and others, prepared a paper [Ref. 5] describing a computer program entitled Numerical Electromagnetics Code for analyzing the electromagnetic response of an arbitrary structure consisting of wires and surfaces in free space or over a ground plane.

Before the advent of the computer, electromagnetic problems were formulated in terms of partial differential equations with boundary conditions or in terms of an integral equation. Much work was needed to apply these classical methods to practical problems and only antennas with simple geometries could be treated.

With the Method of Moments, the integral equation for the antenna current is replaced with a matrix equation and then solved.   Computer codes such as NEC and MININEC now enable the analysis of very complicated antenna systems and provide answers to a good degree of accuracy. NEC requires a main-frame computer for efficient implementation.   MININEC was written in BASIC for PC's.   The NEC and MININEC have taken the electromagnetic community "by storm" because of their great versatility and applicability. With these codes the antenna enginneer can test different approaches to design problems and can explore new trends and concentrate on his immediate problems without getting involved with the complications of classical elctromagnetic theory.   A good fundamental knowledge of electromagnetics, some familiarity with methods and limitations of the antenna computer code, and a certain experience with NEC for known cases, including the ability to validate answers from the code, are important requirements for the engineer.

Numerical Electromagnetics Code (NEC)-Method of Moments
is a paper of G.J.Burke and A.J.Pogio [Ref. 7] published in
1981, describing a user-oriented computer code for analysis
of the electromagnetic response of antennas and other metal
surfaces.

A.   SLOT ANTENNAS

   1.   <u>The Principle of Slot Antennas</u>

         Slot antennas may be cut in a metallic surface such as the bulkhead of a ship, the skin of an aircraft or the wall of a waveguide. The slot may be fed by a transmission line or a generator connected across it. In this paper a single generator is used to feed the slot antenna.

         The antenna built with two resonant stubs of quarter wavelength connected to a 2-wire transmission line (Fig. 2.1) forms a poor radiator. If the lines are spaced very close and carry currents of opposite phase, their fields cancel one each other. The end wires carry currents in same phase but they are too short to radiate efficiently.
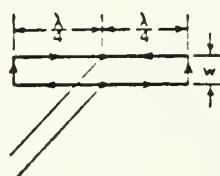
Figure 2.1   Poor Radiator.

         But now the antenna shown in Fig. 2.2 can be considered as a very efficient radiator.

14
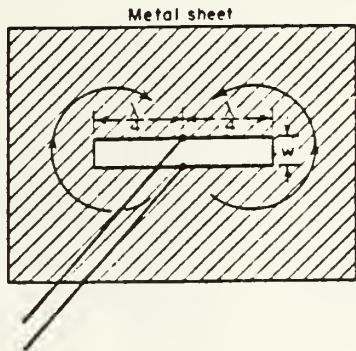
Figure 2.2   Efficient Slot Radiator.

This is a slot antenna. The currents are spread out all over the conducting surface and there is radiation from both sides. For horizontal slots the radiation perpendicular to the sheet is vertically polarized. The input impedance is about 500 ohms for a resonant slot of half wavelength fed at its center. It is possible to decrease the input impedance with an off-center feed point. For a coaxial cable of 50 ohms this offset distance should be about $S=1/20$ of the wavelength as seen in Fig. 2.3.

As was stated before, the conducting sheet radiates equally from both sides, but if a very large boxed sheet is placed at one side of the slot, the radiation will occur only from one side (see Fig. 2.4).

If the depth of the box placed behind the slot is about one fourth wavelength, there will be no susceptance at the terminal of the slot and the slot input impedance should be 1000 ohms [Ref. 8].
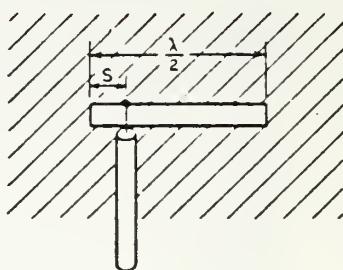
Figure 2.3   Special Feeding.
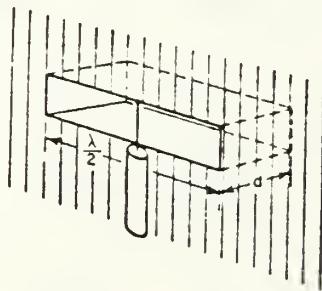
Figure 2.4   Boxed Slot.

2.   <u>Radiation</u> <u>Pattern</u> <u>of</u> <u>Slots</u>

Booker [Ref. 9] showed that a slot radiation pattern
is   the   same   as   that   of   a   complementary   horizontal

half-wavelength dipole (see Fig. 2.5) consisting of a perfectly conducting flat strip of same width.
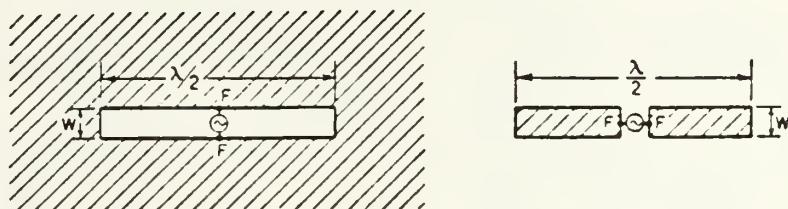
Figure 2.5   Complementary Pair.

But there are two differences:
- the electric and magnetic fields are interchanged and
- the component of the electric field of the slot normal to the sheet is discontinuous from one side to the other, the direction of the field reversing. The same thing happens with the tangential magnetic field.

The infinite flat sheet is coincident with x-z plane and the long dimension of the slot is in the x-direction (see Fig. 2.6).

The radiation-field pattern has the same doughnut shape but the direction of E, for example, is interchanged if compared with that of the complementary dipole antenna coincident with x-axis.

3.   The Impedance of Slot Antennas

By using Babinet's principle, many of the problems of slot antennas can be reduced to situations involving complementary linear antennas for which solutions have already been obtained.

17
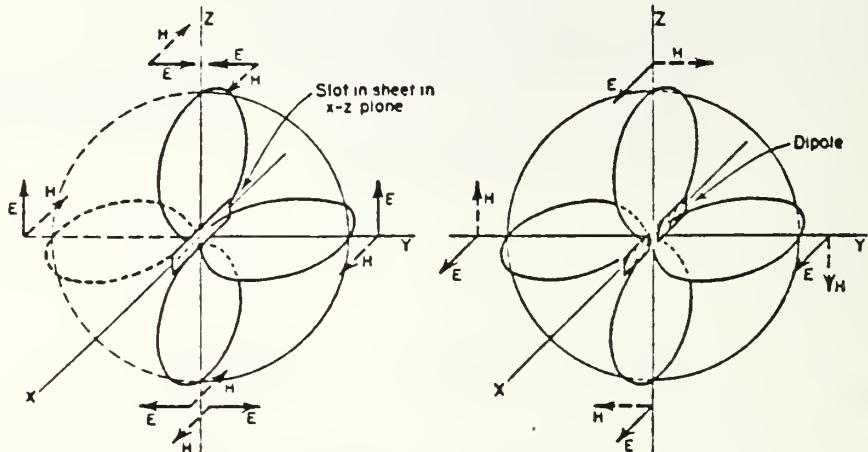
Figure 2.6   E-Field Radiation Pattern.

Kraus   showed how to develop a relation for the impedance Zs of a slot antenna in terms of the impedance Zd of a complementary dipole antenna.

Since Zd may be complex:

$$Zs = Zo^2 /4Zd = 376.7^2/4(Rd + jXd) = \qquad (eqn\ 2.1)$$

$$= 35,476(Rd - jXd)/(Rd^2 + Xd^2)$$

18

It can be easily seen that if the dipole antenna is inductive, the slot is capacitive and vice-versa.

Lengthening a half wavelength dipole makes it more inductive, but lengthening a half wavelength slot makes it more capacitive.

Kraus gives some numerical examples that will be used later on comparing with NEC results:

- the terminal impedance of an infinitesimally thin half wavelength slot antenna is:

$$Zs = 35,476/(73 + j42.5) = 363 - j211 \text{ ohms} \qquad (\text{eqn } 2.2)$$

- the terminal resistance of the complementary slot antenna compared to that of a cylindrical antenna with length-to-diameter (L/D) ratio of 100 and length of about 0.475 wavelengths is:

$$Zs = 35,476/67 = 530 \text{ ohms} \qquad (\text{eqn } 2.3)$$

- the terminal resistance of a complementary slot antenna compared to that of a cylindrical dipole with L/D=28 and length of about 0.925 wavelengths (Zs = 710 ohms) is about 50 ohms, which could be easily matched to a 50 ohms-coaxial cable.

Finally it must be said that:

- if the slots are enclosed on one side of the sheet with a box of such size that zero suceptance is shunted across the slot terminals, due to the box, the impedances are doubled;

- the bandwidth (BW) or selectivity of a slot antenna are the same as for a complementary dipole. If a slot is widened (smaller L/W ratio), the slot antenna BW is increased the same as increasing the thickness of a dipole antenna (smaller L/D ratio) increases its BW; and,

- this study applies to slots in infinite sheets. The impedance values are the same provided that the edge of the sheet is at least a wavelength from the slot.

B.   PRELIMINARY CONSIDERATIONS: BOUNDARY CONDITIONS

It is worthwhile to review some ideas about boundary conditions which are considered by NEC when dealing with wire structures.

Two main considerations are assumed in this study:

- the flat surface of a real bulkhead was modeled by the wire grid; and

- the slot opening was outlined by wires.

These assumptions produce, for example, near fields inside the slot and currents on the wire grid which can be an acceptable approximation to the real slot placed in a solid planar surface. The differences are in the nature of concentration of currents along the wires of the grid as opposed to a smoother surface current distribution of a plate. The near field plot shown in Chapter V is an evidence of that fact.

III. A BRIEF DESCRIPTION OF NEC

Numerical Electromagnetics Code, NEC, is a computer program that analyzes the electromagnetic response of antennas. It computes a numerical solution to integral equations that describe the currents induced on a structure by voltage or current generators or incident fields.

NEC was developed by Lawrence Livermore Laboratories with funding from the Naval Electronics Systems Command.

A. MAIN CHARACTERISTICS OF NEC

An Integral Equation (I.E.) for current modeling on thin wires is combined with an I.E. for modeling the current on smooth surfaces to describe the electromagnetic response of an arbitrary structure. The structure may have active parts, may be located over a perfect or imperfect ground plane, and may have distributed or lumped-element loading. The excitation may come from voltage or current sources on the structure, an incident plane wave with linear or elliptic polarization, or the field may be due to a elementary dipole. The outputs may include current and charge density, power gain or directive gain, near or far electric or magnetic fields, impedance or admittance, total radiated power or input power.

NEC utilizes the Gauss-Doolittle Method for solving the matrix equations generated by the Method of Moments when solving the I.E.'s.

It is a discrete sampling code where a complex structure must be dissected into a number of simple elements, which are thin wires or small surface areas, to which the Electric Field Integral Equation (EFIE) or the Magnetic Field Integral Equation (MFIE) are applied, respectively when using the approximations. The resemblance with the real

21

world is strongly influenced by the choice of the discretization of the structure by the user. Smaller geometric elements produce models which come close to reality. But, the smaller the elements, the larger the number of elements will be, which means the larger the matrix of equations and hence the more expensive the solution will be.

The choice of proper dissecting is gained with experience and becomes an art as well as a science.

Generally, segment lengths (Δ) should be less than 0.1 wavelength [Ref. 6]. Shorter segments (0.05 wavelength) may be needed at curves or junctions. Segments smaller than 0.001 wavelength should be avoided. The radius of the wire "a" relative to the wavelength depends on the Kernel used in the I.E.. There are two options. The thin wire kernel models a filament current, while the extended Kernel models a uniform current distribution around the segment surface. The field of the distributed current is approximated by the first two terms in a series expansion of the exact field, in powers of a^2. The first term (a^0) is identical to the thin wire kernel; the second term extends the accuracy for larger values of a. Both kernels incorporate the thin wire approximations and both also require that the ratio between the wire perimeter and the wavelength be much less than 1. The thin wire kernel requires a ratio $\Delta/a > 2$. These values ensure errors are less than 1%. It must be said that the extended kernel also permits a value of $\Delta/a > 2$.

The conducting surfaces [Ref. 10] are modeled by small flat surface patches which conform as closely as possible to curved surfaces. The parameter defining a patch is a normal unit vector, originating from the center of the patch, defined in cartesian coordinates. Each patch which connects to a wire have the connection point at the patch center. The code divides each patch into 4 equal patches about the

wire end, along the unit vector lines describing the surface
of the patch. An interpolation function is applied to the 4
patches to represent placement of the current onto the
patches and the function is numerically integrated. Patches
with wires connected to them should be chosen to be
approximately square with sides parallel to the unit vectors
defining the surface. Only one wire may connect to a patch
and it may not lie in the plane of the patch. A minimum of
about 25 patches should be used per wavelength of surface
area; the maximum size for an individual patch is about 0.04
square wavelengths. Long narrow patches should be avoided.

For a perfectly conducting ground, the code generates a
reflected image. Structures may be close to, or contact, the
ground plane.

The EFIE is used for thin wire structures with small
conductor volume. It is derived from the electric field
representation for a current distribution confined to the
surface of a perfectly conducting body and is solved in NEC.
The MFIE is derived from the integral representation for
the magnetic field of a closed surface current distribution
and is also solved in NEC.

B.   METHOD OF MOMENTS

The Method of Moments is a technique whereby an integral
or differential equation is reduced to a system of linear
algebraic equations which are easily manipulated by high
speed digital computers. Therefore its objective is the
conversion of a continuous problem into a discrete problem
having a finite number of unknowns.

References [10] and [11] discuss the method showing that
the accuracy of solution depends on the choice of basis
function or, in other words, upon both resolution of the
discretizement (no. of unknowns) and also upon the method of
approximating the continuous solution and how the equation
is enforced. To generate the system of linear equations,

23

the structure is divided into a number of segments. The current distribution on the antenna is approximated as the summation of currents found on each segment. The next step is the identification of a set of weighting functions. These are set equal to the basis functions, when using Galerkin's Method. In NEC weighting functions are chosen as a set of Dirac Delta functions for efficiency of solution. The system of equations is then solved for the exact value at match points and a very close approximation to the actual current distribution at nearby points can be obtained.

After determining the currents the other non-zero scalar field components can be computed.

C. THIN WIRE APPROXIMATION

For a thin perfect electrical conductor cylinder with radius "a" and length "L", where a << one wavelength and a << L, and in presence of a known incident field it is possible to assume that induced vector surface current, Js , is only z-directed and resides on the surface.

The following thin wire approximations were used:
- transverse currents can be neglected relative to axial currents on the wire;
- the current can be approximated by filaments at the geometrical center the wire axis;
- electrical field consists of both incident and scattered fields. As the induction theorem states that the induced surface current density must produce an electric field whose tangential component cancels that of the incident electric field, on the surface of the body, the boundary condition on the electric field need to be inforced in the axial direction only;and
- the circumferential variation in the axial current can be neglected and the current at the ends of cylindrical surfaces is approximately zero.

D. NUMERICAL GREEN'S FUNCTION

The Numerical Green's Function (NGF) option is used in this paper. A fixed structure and its environment are modeled and the factored interaction matrix is saved in a file. New parts are added to the model in subsequent

computer runs and the complete solution obtained without repeating calculations for the data on file. The main purpose of the NGF is to avoid unnecessary repetition of calculations when a part of the model, such as the simulation of the bulkhead and the slot using the wire grid model, is modified just by adding a feed segment one or more times while the environment remains constant. The self-interation matrix for the fixed environment may be computed, factored for solution, and saved on a tape or disk file. Solution for a new feed point, for example, then requires only the evaluation of the self-interation matrix for the fed segment, the mutual antenna-to-bulkhead interations, and matrix manipulations for a partitioned-matrix solution.

Another reason for using the NGF option is to exploit partial symmetry in a structure, which was done in this paper. Such partial symmetry may be exploited to reduce solution time by running the symmetric part of the model first and writing a NGF file. The unsymmetric parts may then be added in a second run.

The use of NGF in this paper during the simulations of large, time-consuming models saved expensive results for further use. Without adding new wires they were used with new excitation, or to compute new radiation patterns, or near field.

IV. MODEL DESCRIPTION

Using NEC geometry cards, the first step of this investigation was to build, with wires, a bulkhead of a ship where a slot antenna was placed.
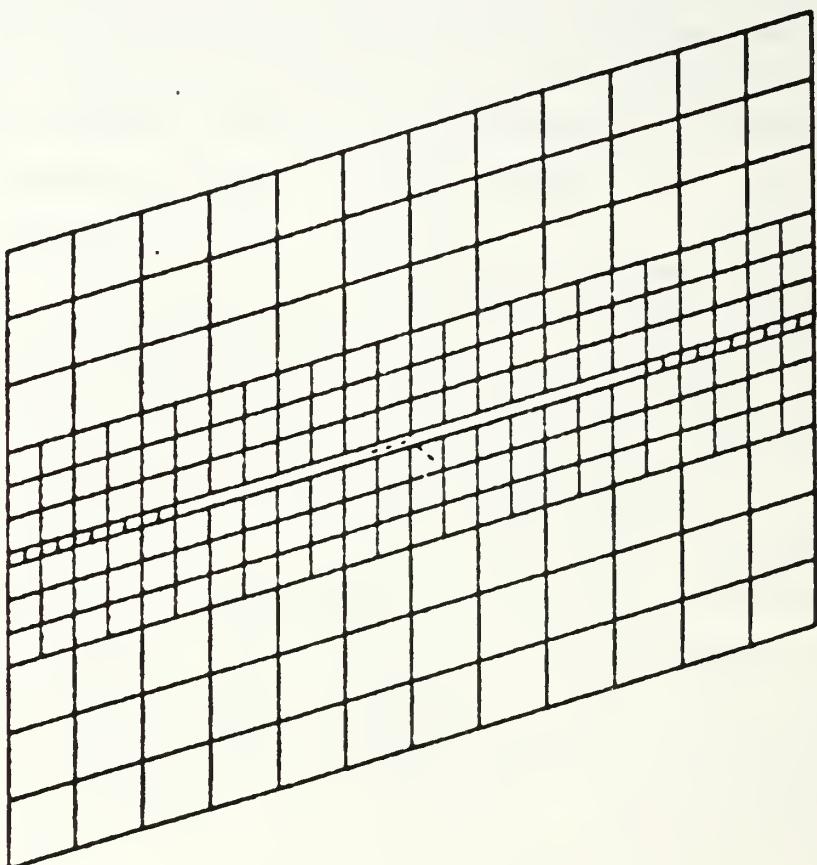
**THETA = 60.00 PHI = 60.00 ETA = 90.00**

Figure 4.1   Bulkhead with Slot Antenna.

Thus,   the wire-grid   modeling ability of NEC is used   to simulate the behavior of a rectangular slot antenna.

Fig. 4.1 shows the bulkhead wire-grid model with dimensions 12m x 9.2m in the center of which was placed a slot with dimensions 7m x 0.2m. These are typical bulkhead dimensions for river patrol boats or small corvettes. A simple rectangular slot cut into a square conducting sheet was chosen as the antenna structure to be evaluated using the wire-grid modeling approach. This geometry simplifies the modeling procedure and , as shown in Chapter II , there is some qualitative information available regarding the characteristics of rectangular slot antennas.

```
CE BULKHEAD WITH SLOT ANTENNA
GW 1.1. -6.0.4.6. -6.0.3.6. .01
GW 2.1. -6.0.4.6. -5.0.4.6. .01
GM 2.11. 0.0.0. 1.0.0
GW 25.1. 6.0.4.6. 6.0.3.6. .01
GM 25.2. 0.0.0. 0.0.-1
GW 76.1. -6.0.1.6. -6.0.1.1. .01
GW 77.1. -6.0.1.6. -5.5.0.1.6. .01
GM 2.23. 0.0.0. .5.0.0. 76.77
GW 124.1. 6.0.1.6. 6.0.1.1. .01
GM 49.2. 0.0.0. 0.0.-.5. 76.124
GW 223.1. 3.5.0..1. 3.5.0.0. .01
GW 224.1. 3.5.0..1. 3.75.0..1. .01
GM 2.9. 0.0.0. .25.0.0. 223.224
GW 243.1. 6.0..1. 6.0.0. .01
GM 21.1. 0.0.0. -9.5.0.0. 223.243
GW 265.1. -3.5.0..1. -3.0..1. .01
GW 266.1. -3.0..1. -2.5.0..1. .01
GM 2.6. 0.0.0. 1.0.0. 265.266
GX 278.001
GE
FR 0.0.0.0. 20.357
WG
EN
```

Figure 4.2   NEC Geometry Cards.

A sample of the NEC data used to simulate the slot and the bulkhead is shown in Fig. 4.2.

To produce the Numerical Green's Function (NGF) of this slot the data set shown in Appendix A was first runat a frequency of 20.357 MHz the half-wavelength resonant frequency of the slot.

It was mandatory to use the MVS (Multiple Virtual System) because the great majority of jobs were class C or G (CPU times per job of 3 minutes and 15 minutes , respectively).

THETA = 60.00 PHI = 60.00 ETA = 90.00
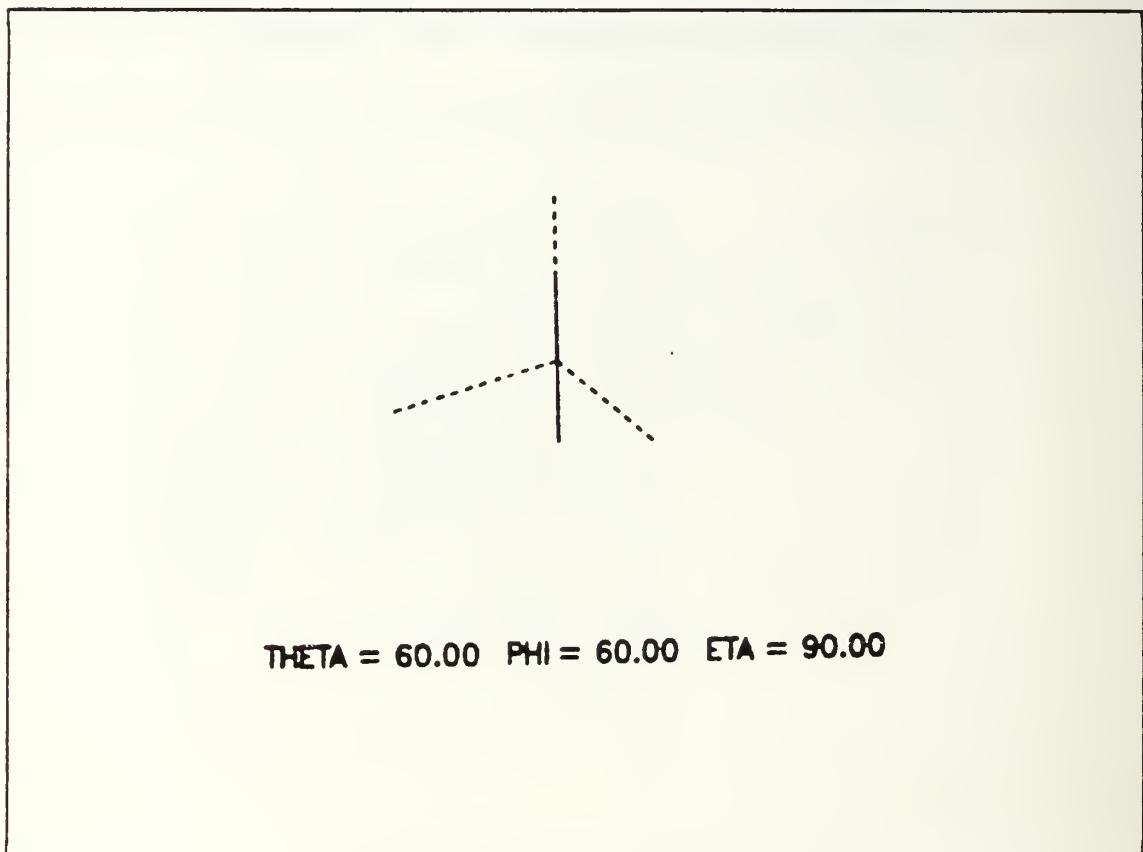
Figure 4.3   Wire Segment Used for Feeding the Slot.

The next step was to feed the slot at different points along x-axis (from x=0.0m through x=3.0m in 0.5m steps) and to analyze its radiation patterns (vertical and horizontal) for E-field, its input impedance and to plot the near field inside the antenna.

28

Fig. 4.3 shows the segment used to feed the structure oriented in the X-Y-Z coordinate system.

Other data sets were developed to study the change of the slot input impedance with frequency variation. New NGF's had to be calculated for 5MHz, 10MHz and 30MHz.

The slot width (w) was varied and the bandwidth (BW) performance studied.
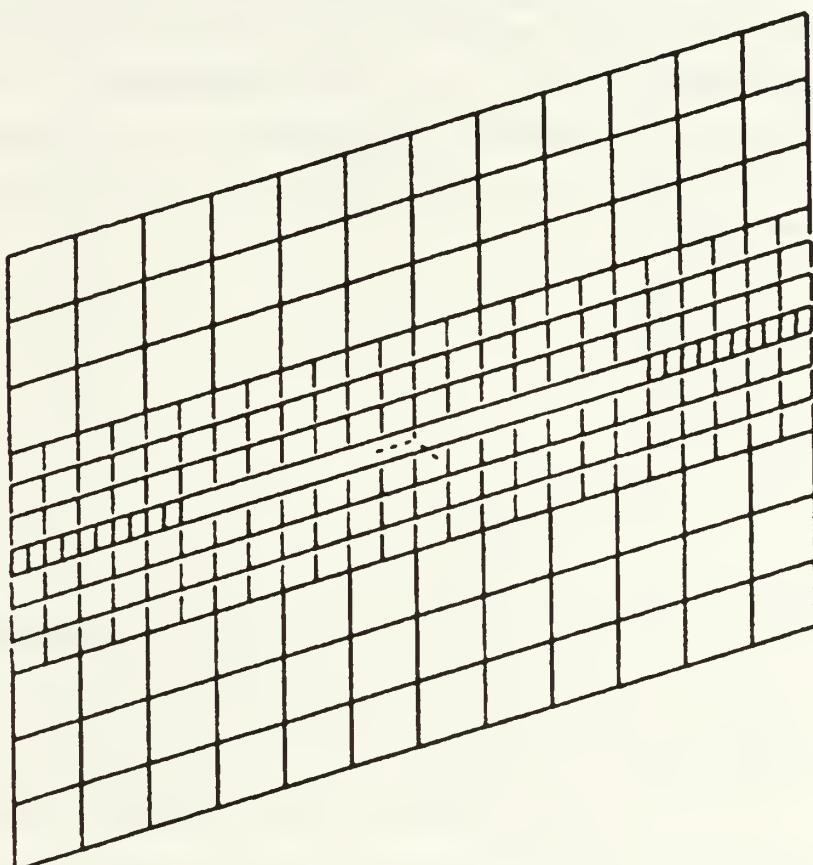
THETA = 60.00 PHI = 60.00 ETA = 90.00

Figure 4.4   New Wire-Grid Model for w=0.4m.

Figure 4.4 shows the new wire-grid model with w=0.4m.

After feeding the two structures at the same seven points as for w=0.2m, a comparison gave more information about the BW performance of these slot structures as "w" is varied.

Values of input impedance were also included for the case where w=0.5m.

Keeping the same feed point (at x=0.0m), a comparison between the input impedance for "w" =0.2 and 0.4m, and four frequencies (5,10,20 and 30 MHz) was made.

Finally, impedance is presented for frequencies between 18 and 22 MHz, in 1 MHz steps, for both slots with w=0.2m and w=0.4m.

V. <u>NUMERICAL RESULTS</u>

A.   INPUT IMPEDANCES

TABLE I	
SLOT INPUT IMPEDANCE: F=20 MHZ AND W=0.2M	
Distance "x" (meters)	Impedance (ohms)
0.0	464 - j 126.5
0.5	443 - j 113.7
1.0	385.9 - j 78.58
1.5	300.6 - j 29.57
2.0	202.2 + j 20.59
2.5	107.6 + j 57.1
3.0	34.2 + j 63.63

Seven data sets were run to evaluate the variation of input impedance of the slot as a function of "x", the feedpoint location along the horizontal axis.

These results are shown on two different curves, one for resistance and the other for reactance, in Figures 5.1 and 5.2. Table I contains the plotted values.

The point along x-axis where one would expect an input impedance of 50 ohms matched the theoretical value of Chapter II. In Fig.5.1, for example, it can be seen that for an input resistance of 50 ohms the value of "x" is close to 2.88m, which matches the theory. One should notice that:

$$x = 3.5 - (\lambda/20) = 3.5 - (300/20.357/20) = 2.763m$$

31
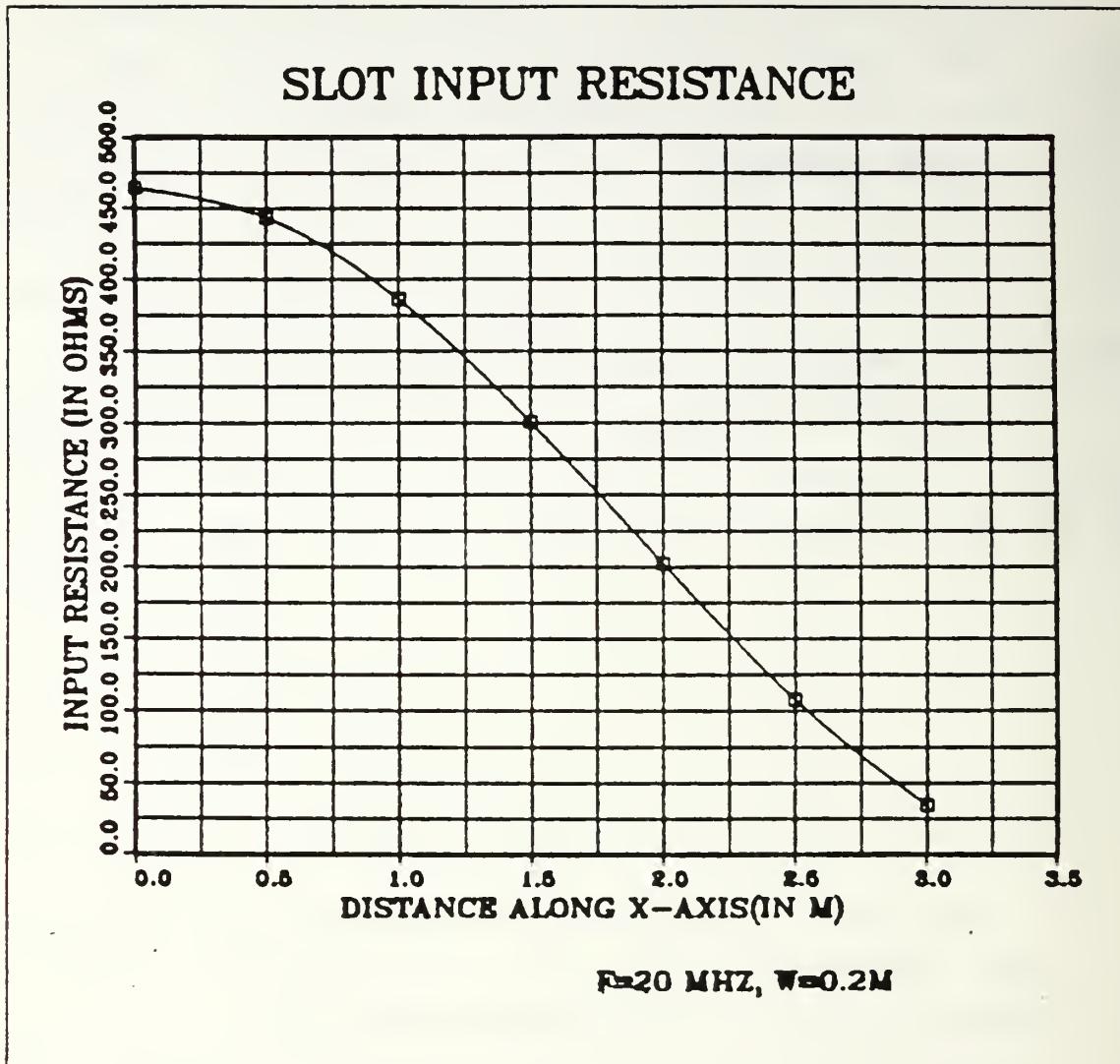
Figure 5.1   Input Resistance-20 Mhz.

In Fig. 5.2 it is easily seen that resonance is at a feed position of x=1.8m.

The same procedure was repeated for f=5 MHz as can be seen in Appendix B.

For 10 MHz and 30 MHz, the results appear respectively in Appendices C and D.

Table II contains impedance results for w=0.2m and feeding distance of x=0.0m.

32
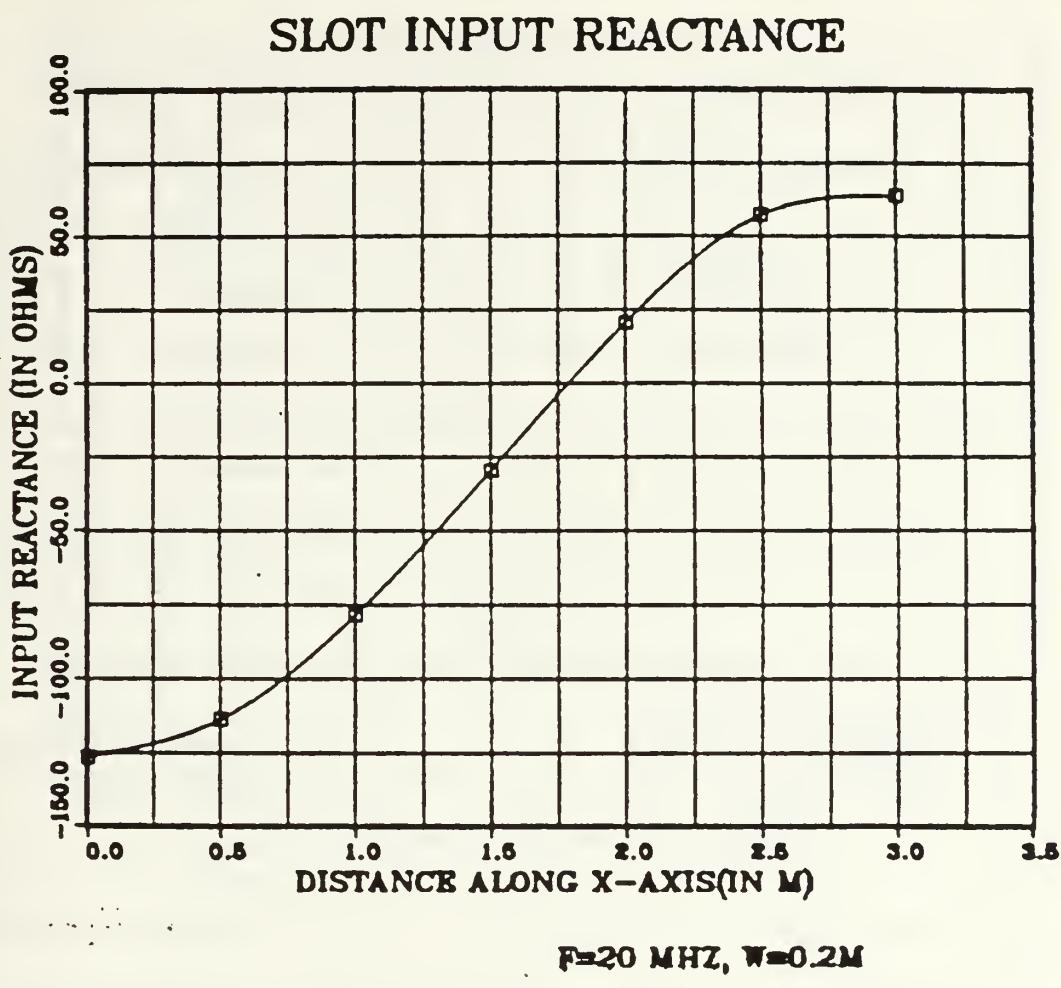
Figure 5.2   Input Reactance-20 Mhz.

Table III contains results for w=0.4m and feeding distance of x=0.0m. Here, the slot width is twice that of the previous case.

TABLE II

SLOT IMPEDANCE(X=0.0M AND W=0.2M): 5 TO 30MHZ

Frequency (MHz)	Impedance(ohms)
5.0	0.028 + j 55.18
10.0	7.25 + j 142.0
20.0	464.0 - j 126.5
30.0	74.3 - j 37.9

TABLE III

SLOT IMPEDANCE(X=0.0M AND W=0.4M): 5 TO 30MHZ

Frequency (MHz)	Impedance(ohms)
5.0	0.253 E-3 + j 111.44
10.0	0.263 E-1 + j 263.8
20.0	1105.1 - j 7928.7
30.0	5.31 - j 267.0

B. BANDWIDTH PERFORMANCE

As explained in Chapter IV, the first task in this study was a comparison between both models (w=0.2m and w=0.4m), keeping the frequency (f=20.0 MHz) constant.

The results are in Fig. 5.3 and 5.4 where we see that for w=0.2m the input resistance and reactance both have smaller variation than those for w=0.4m. Thus there is an advantage in using the antenna with w=0.4m over that with w=0.2m : a larger range of input impedances is available to work with.
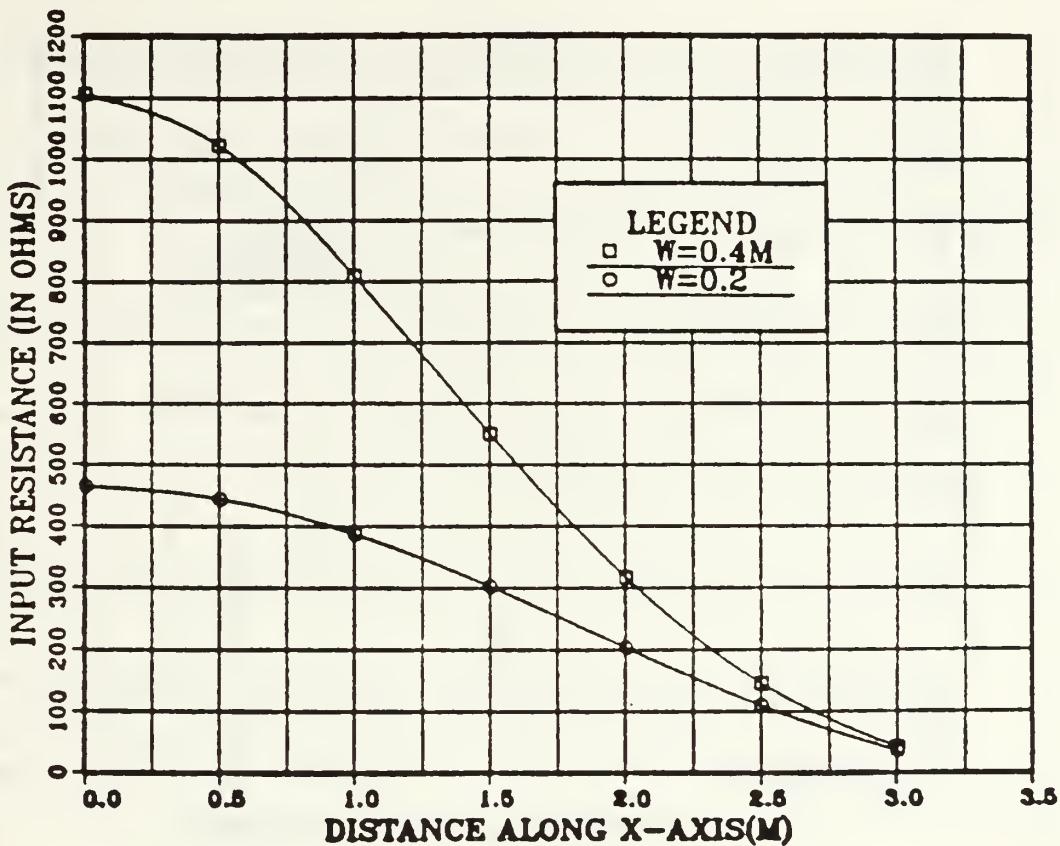
Figure 5.3   Slot Resistance Variation-20 MHz.

Also included are two plots for w=0.5m, f=20MHz, one for the input resistance and the other for the input reactance, in Appendix E.

Another possible parameter variation is with frequency, keeping the feed point location (x=0.0m) fixed, and studing the behavior of input impedance for the same slot width. This was done for 18 MHz to 22 MHz in steps of 1 MHz, for both cases where w=0.2m,x=0.0m (Table IV) and w=0.4m,x=0.0m (Table V).

Both plots corresponding to these tables are shown in Fig. F.1 and Fig. F.2 It is easy to see that for the first
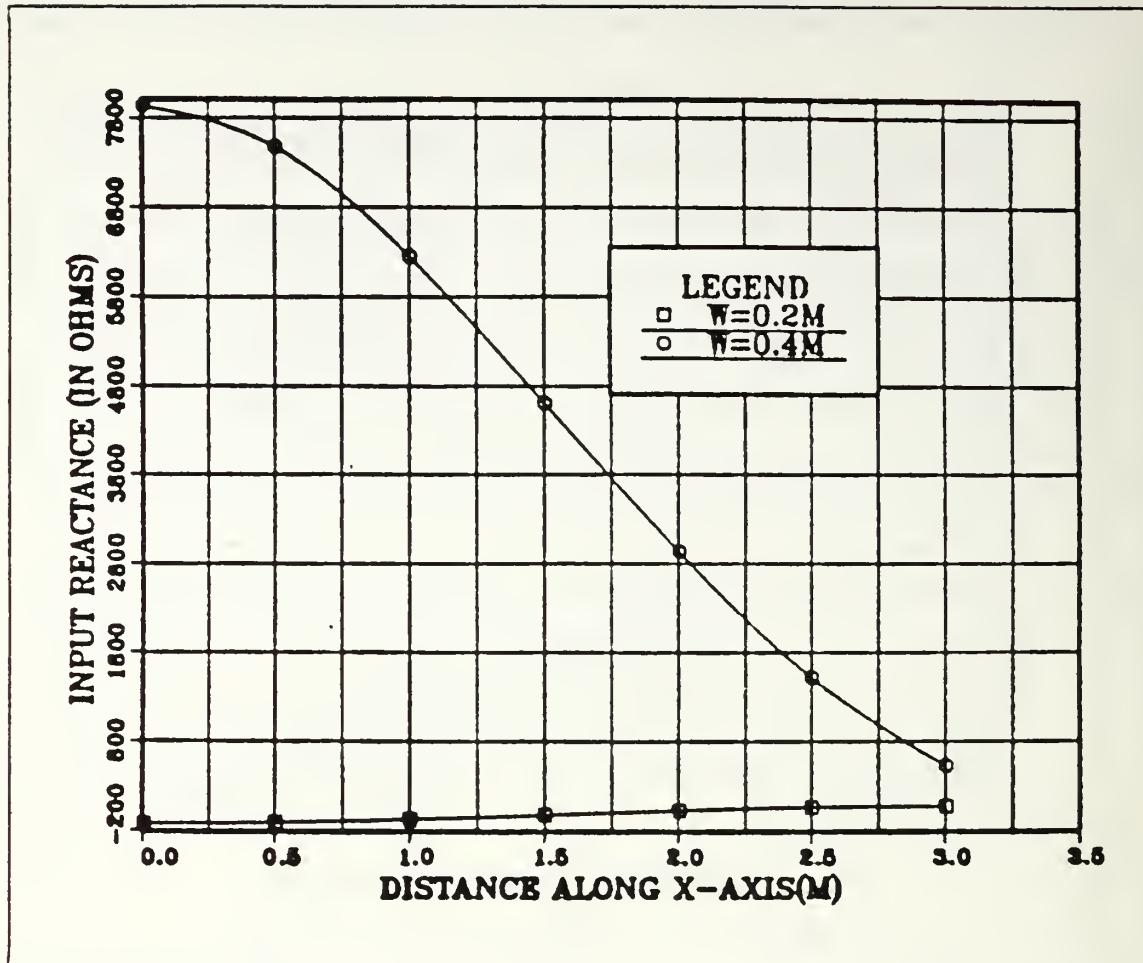
Figure 5.4   Slot Reactance Variation-20 MHz.

value of w=0.2m the resonance is close to 19 MHz, while for w=0.4m the resonance can be found at f=20.4 MHz, approximately. Thus one can say that the resonant frequency does not depend greatly on the slot width.

C.   NEAR FIELD INSIDE THE SLOT

The results of the near-field inside the slot for z=0.0m are shown in Fig.5.5 .

Referring to the geometry of Fig. 4.1, for z=0.05m E-peak field is calculated just over the middle of the slot. The calculations were repeated for z=0.0m and z=0.075m as shown in Appendix G.

36

TABLE IV

SLOT IMPEDANCE(X=0. OM AND W=0. 2M): 18 TO 22MHZ

Frequency (MHz)	Impedance(ohms)		
18. 0	434. 1	+ j	279. 2
19. 0	539. 4	+ j	125. 7
20. 0	464. 0	- j	126. 5
21. 0	373. 3	- j	179. 5
22. 0	248. 1	- j	182. 4

TABLE V

SLOT IMPEDANCE(X=0. OM AND W=0. 4M): 18 TO 22MHZ

Frequency (MHz)	Impedance(ohms)		
18. 0	2. 57	+ j	1261. 2
19. 0	58. 52	+ j	4124. 0
20. 0	1105. 1	- j	7928. 7
21. 0	1961. 8	- j	11681. 0
22. 0	95. 44	- j	2546. 0

It was taken into account, for sake of simplification, that the field is symmetric with respect to the y-axis.

The E-peak is a composite of Ex and Ez components, with Ez being the dominant component. The smooth decline of E-peak along the x-direction can be observed in Fig. 5.5 and Appendix G.

There are some points of maximum along the near E-field curve as seen in Fig. 5.5. These points are exactly those where the junctions of the segments occur along the upper

37

NEAR E-FIELD INSIDE SLOT
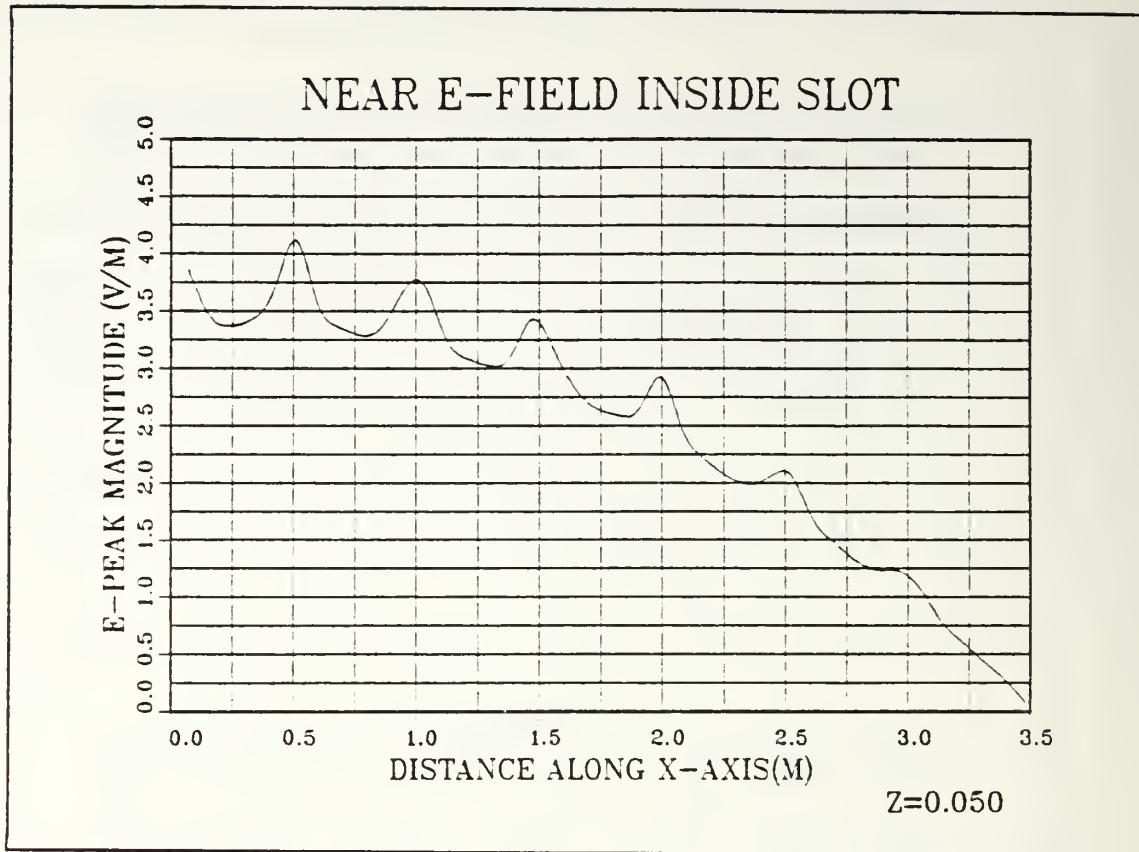
Figure 5.5   Near E-Field for z=0.050m.

and lower wires of the larger sides of the slot, because the flat surface of the real bulkhead is modeled here by the wire grid.

D.   RADIATION PATTERNS

1.   Single Voltage Source

The radiation pattern plots agreed with slot antenna theory.

For w=0.2m and f=20.0 MHz, two horizontal patterns (one for x=0.5m and the other for x=3,0m) and two vertical patterns (for the same feeding points along x-axis) were plotted. Appendix H contains these plots.

38

2.   <u>Multiple</u> <u>Voltage</u> <u>Sources</u>

One additional test with the same model (w=0.2m and f=20.0MHz) was considered.

The slot   pattern   was   not very   sensitive   to increasing the number of multiple feed segments. Appendix I shows this (horizontal patterns only)   for three, nine and thirteen segments fed simultaneously. Very little change in shape is noted.

Appendix J shows the NEC geometry card data set for multiple feeding using thirteen voltage sources.

VI. <u>CONCLUSIONS</u> <u>AND</u> <u>SUGGESTIONS</u>

It has been shown that two main characteristics of a
slot antenna were produced in this numerical modeling study.
These were the antenna's terminal impedance and its
radiation pattern. For the simulated slot antenna, the
terminal impedance is the impedance seen by the voltage
source used to excite the antenna. This investigation
produced good results and, as said before, this impedance is
important with regard to matching the antenna to a
transmission line and a source or receiver to assure
efficiency in the transfer of power. The point along x-axis
where one would expect an input impedance of 50 ohms matched
the theoretical value of Chapter II. For "x" approximately
equal to 2.88m, the input impedance was about 50 ohms. The
resonance is at feed position of x=1.8m and, for that point,
the input resistance is about 240 ohms.

The feed point is not the only parameter affecting the
computer model's impedance. The slot width variation led to
a conclusion that there is an advantage in using antennas
with broader "w" on account of having a larger range of
input impedances to work with.

Another possible parameter variation, keeping the feed
point location fixed, is in frequency. Testing over the
frequency range: 18 to 22 Mhz, it was verified that the
resonance does not depend greatly on the slot width. For
both models with w=0.2m and w=0.4m, the resonant frequency
was around 19 MHz and 20.4 MHz, respectively.

The radiation pattern defines the directional gain of an
antenna. In this thesis the spatial distribution of the phi-
and theta-polarized electric field components radiated in
the far-zone of antenna as well as near-fields were
investigated. Both calculations agreed with the slot

antenna theory keeping in mind that the group of points of maximum values appeared because a wire grid is only an approximation to a planar surface for currents on that surface.

One suggestion is to place some type of dielectric backing in the slot region [Ref. 13], both for structural support and to seal against the environment. Therefore, it would be useful to develop a method for the wire-grid model to account for the presence of a slot dielectric.

Another suggestion is to try some computation with boxed-in slot antennas and study their expected unidirectional radiation patterns. Another investigation is to perform a more detailed study of the influences of the slot width variation on bandwidth.

In the same above reference, on page 7, Funke took into account, for sake of more accuracy, the "wire mesh density". This term actually deals with the length of the wire segments which form the grid for the modeled surface. He asked how tight must the mesh be in order to obtain reasonable results from the model. It must not be forgotten that the penalty for a tight mesh with very short wire segments is large computer storage area and long execution time.

In this study, 556 segments were used (not including one required segment to represent the voltage source which feeds the slot antenna). Funke also began his investigation with a 555 segment model and showed that very little change in the calculated impedance was observed for 641 and 683 segment wire-grid models. Decreasing the wire mesh density, the results were almost the same with a 383 segment model which would be a good start for further studies in this subject.

From the results of Chapter IV and V it can be said that NEC is an effective analysis tool for some slot antenna

calculations, and should be further used in the application of low profile HF shipboard antenna designs.

APPENDIX A

AN EXAMPLE OF JOB STREAM WITH NGF DATA SET

```
//S3        JOB (1714,1234),'NEC RUN',CLASS=G
//NEC        PROC VERSION=NPSNEC,STORAGE=1024K
//*NEC       PROC VERSION=NPS1000,STORAGE=2048K
//GO        EXEC PGM=&VERSION,REGION=&STORAGE
//STEPLIB  DD DISP=SHR,DSN=MSS.F1595.NEC.LOAD
//FT01F001 DD DUMMY
//FT04F001 DD UNIT=SYSDA,SPACE=(CYL,(8,2)),
//            DCB=(RECFM=VS,BLKSIZE=19069)
//FT05F001 DD DDNAME=SYSIN
//FT06F001 DD SYSOUT=*
//FT08F001 DD DUMMY
//FT11F001 DD UNIT=SYSDA,SPACE=(CYL,(8,2)),
//            DCB=(RECFM=VS,BLKSIZE=19069)
//FT12F001 DD UNIT=SYSDA,SPACE=(CYL,(8,2)),
//            DCB=(RECFM=VS,BLKSIZE=19069)
//FT13F001 DD UNIT=SYSDA,SPACE=(CYL,(8,2)),
//            DCB=(RECFM=VS,BLKSIZE=19069)
//FT14F001 DD UNIT=SYSDA,SPACE=(CYL,(8,2)),
//            DCB=(RECFM=VS,BLKSIZE=19069)
//FT15F001 DD UNIT=SYSDA,SPACE=(CYL,(8,2)),
//            DCB=(RECFM=VS,BLKSIZE=19069)
//FT16F001 DD UNIT=SYSDA,SPACE=(CYL,(8,2)),
//            DCB=(RECFM=VS,BLKSIZE=19069)
//FT20F001 DD UNIT=SYSDA,SPACE=(CYL,(8,2)),
//            DCB=(RECFM=VS,BLKSIZE=19069)
//FT21F001 DD DUMMY
//        PEND
//STEPNAME EXEC NEC,VERSION=DNPS1000,STORAGE=2048K
//*
//*DIRECT THE FILE 08 OUTPUT DATA
```

43

```
//*TO ITS RESTING PLACE
//*EITHER THE STAGING DISK OR MSS
//*
//*
//*GO.FT08F001 DD DSN=S1714.S3.PLOTDATA,
//*        DISP=(NEW,KEEP),
//*        UNIT=3350,VOL=SER=MVS004,
//*        SPACE=(CYL,(4,4)),
//*        DCB=(LRECL=80,RECFM=FB,BLKSIZE=19040)
//*
//*GO.FT08F001 DD DSN=MSS.S1714.PLOTDATA(S3),
//*        UNIT=3330V,VOL=SER=MS0402,
//*        SPACE=(CYL,(4,4,2)),
//*        DCB=(RECFM=FB,LRECL=80,
//*        BLKSIZE=12960,DSORG=PO),
//*        DISP=(NEW,CATLG)
//*
//*GO.FT08F001 DD DSN=MSS.S1714.PLOTDATA(S3),
//*        DISP=(OLD,KEEP),
//*        DCB=(RECFM=FB,LRECL=80,BLKSIZE=12960,
//*        DSORG=PO)
//*
//*GO.FT08F001 DD DSN=S1714.S3.CURRDATA,
//*        DISP=(NEW,KEEP),
//*        UNIT=3350,VOL=SER=MVS004,
//*        SPACE=(CYL,(4,4,)),
//*        DCB=(LRECL=80,RECFM=FB,BLKSIZE=19040)
//*
//*GO.FT08F001 DD DSN=MSS.S1714.CURRDATA(S3),
//*        UNIT=3330V,VOL=SER=MS0402,
//*        SPACE=(CYL,(4,4,2)),
//*        DCB=(RECFM=FB,LRECL=80,BLKSIZE=12960,
//*        DSORG=PO),
//*        DISP=(NEW,CATLG)
//*
```

```
//*GO.FT08F001 DD DSN=MSS.S1714.CURRDATA(S3),
//*        DISP=(OLD,KEEP),
//*        DCB=(RECFM=FB,LRECL=80,BLKSIZE=12960,
//*        DSORG=PO)
//*
//*NEXT THE NGF FILE LOCATION.
//*EITHER STAGING AREA DISK
//*OR MSS DATA SET.
//*
//*GO.FT20F001 DD DSN=MSS.S1714.NGFDATA(S3),
//*        DISP=SHR,
//*        DCB=(RECFM=VS,BLKSIZE=13030,DSORG=PO)
//*
//*GO.FT20F001 DD DSN=MSS.S1714.NGFDATA(S3),
//*        DISP=(OLD,KEEP),
//*        DCB=(RECFM=VS,BLKSIZE=13030,DSORG=PO)
//*
//*GO.FT20F001 DD DSN=S1714.S3.NGFDATA,
//*        UNIT=3350,VOL=SER=MVS004,
//*              DISP=SHR
//*
//*GO.FT20F001 DD DSN=S1714.FILE.FT20F001,
//*        UNIT=3350,VOL=SER=MVS004,
//*              DISP=SHR
//*
//* C CREATING THE NGF:
//* C CRIANDO A MATRIZ COM A FUNCAO DE GREEN:
//* C CRIANDO NOVA NGFDATA1 PARA CONTER S3
//GO.FT20F001 DD DSN=MSS.S1714.NGFDATA1(S3),
//        UNIT=3330V,VOL=SER=MS0402,
//*       SPACE=(CYL,(4,4,2)),
//        DCB=(RECFM=VS,BLKSIZE=13030,DSORG=PO),
//        DISP=(NEW,CATLG)
//*
//*GO.FT20F001 DD DSN=S1714.S3.NGFDATA,
```

```
//*          DISP=(NEW,KEEP),
//*                UNIT=3350,VOL=SER=MVS004,
//*                SPACE=(CYL,(4,4)),
//*                DCB=(RECFM=VS,BLKSIZE=19040)
//*
//*GO.FT20F001 DD DSN=S1714.FILE.FT20F001,
//*                DISP=(NEW,KEEP),
//*                UNIT=3350,VOL=SER=MVS004,
//*                SPACE=(CYL,(4,4)),
//*                DCB=(RECFM=VS,BLKSIZE=19040)
//*
//*NOW THE SOMMERFELD GRID LOCATION
//*
//*GO.FT21F001 DD DSN=MSS.S1714.SOMDATA(S3),
//*       DISP=SHR,
//*       DCB=(RECFM=VS,BLKSIZE=13030,DSORG=PO)
//*
//*GO.FT21F001 DD DSN=S1714.S3.SOMDATA,
//*       UNIT=3350,VOL=SER=MVS004,
//*                DISP=SHR
//*
//*GO.FT21F001 DD DSN=S1714.FILE.FT21F001,
UNIT=3350,VOL=SER=MVS004,
//*                DISP=SHR
//*
//GO.SYSIN DD *
//* C   INPUT DATA CARDS GO HERE
CE BULKHEAD WITH SLOT ANTENNA
GW 1,1, -6,0,4.6, -6,0,3.6, .01
GW 2,1, -6,0,4.6, -5,0,4.6, .01
GM 2,11, 0,0,0, 1,0,0
GW 25,1, 6,0,4.6, 6,0,3.6, .01
GM 25,2, 0,0,0, 0,0,-1
GW 76,1, -6,0,1.6, -6,0,1.1, .01
GW 77,1, -6,0,1.6, -5.5,0,1.6, .01
```

46

```
GM 2,23, 0,0,0, .5,0,0, 76.77
GW 124,1, 6,0,1.6, 6,0,1.1, .01
GM 49,2, 0,0,0, 0,0,-.5, 76.124
GW 223,1, 3.5,0,.1, 3.5,0,0, .01
GW 224,1, 3.5,0,.1, 3.75,0,.1, .01
GM 2,9, 0,0,0, .25,0,0, 223.224
GW 243,1, 6,0,.1, 6,0,0, .01
GM 21,1, 0,0,0, -9.5,0,0, 223.243
GW 265,1, -3.5,0,.1, -3,0,.1, .01
GW 266,1, -3,0,.1, -2.5,0,.1, .01
GM 2,6, 0,0,0, 1,0,0, 265.266
GX 278,001
GE
FR 0,0,0,0, 5.0
WG
EN
//*
/*
```

# APPENDIX B

SLOT INPUT IMPEDANCE FOR F=5MHZ AND W=0.2M
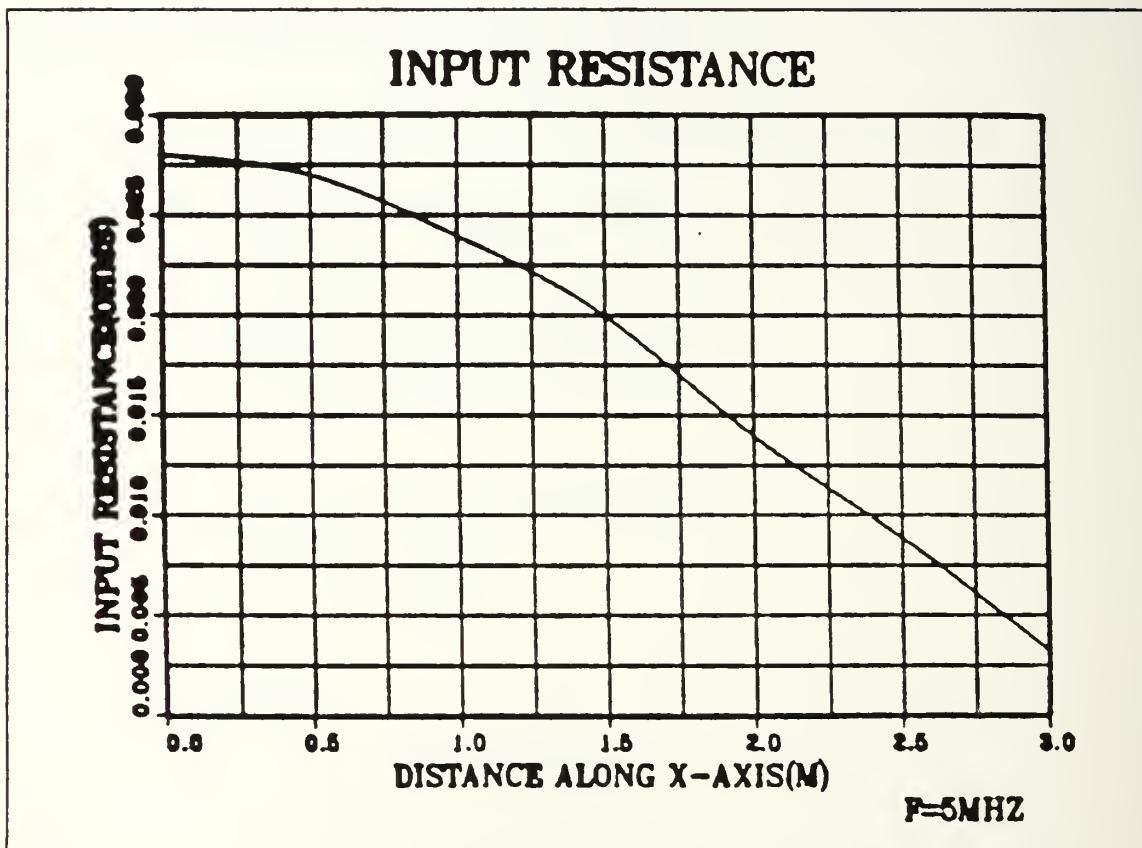
Figure B.1   Input Resistance-f=5MHz and w=0.2m.
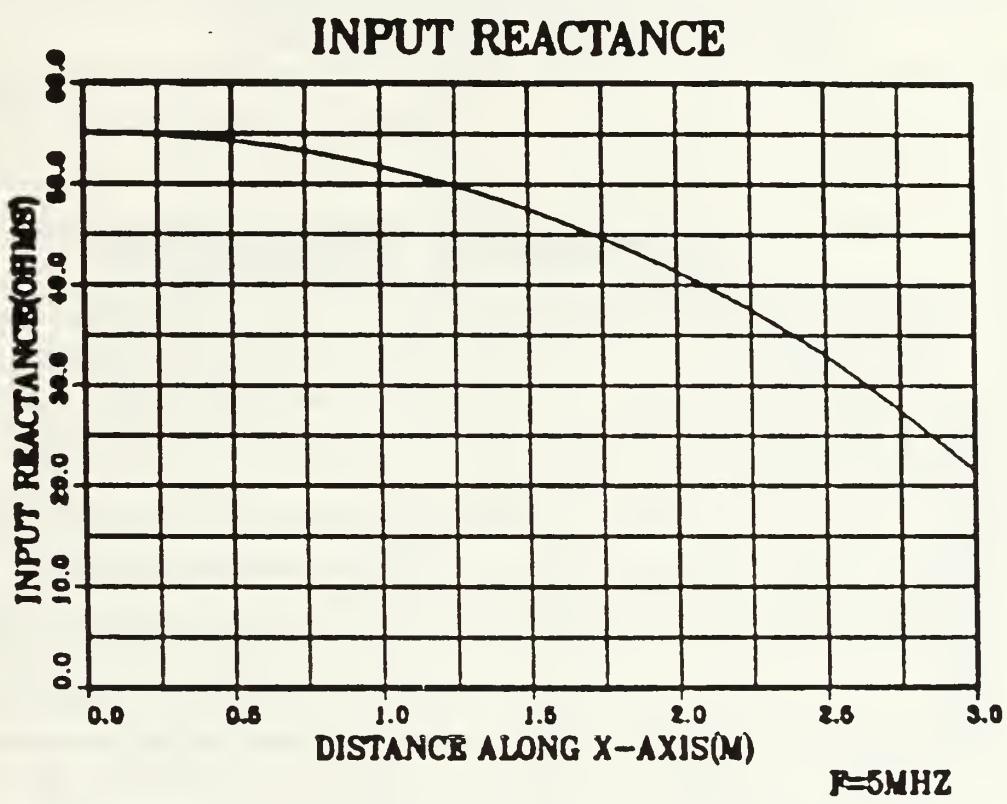
Figure B.2   Input Reactance-f=5MHz and w=0.2m.

APPENDIX C

SLOT INPUT IMPEDANCE FOR F=10MHZ AND W=0.2M
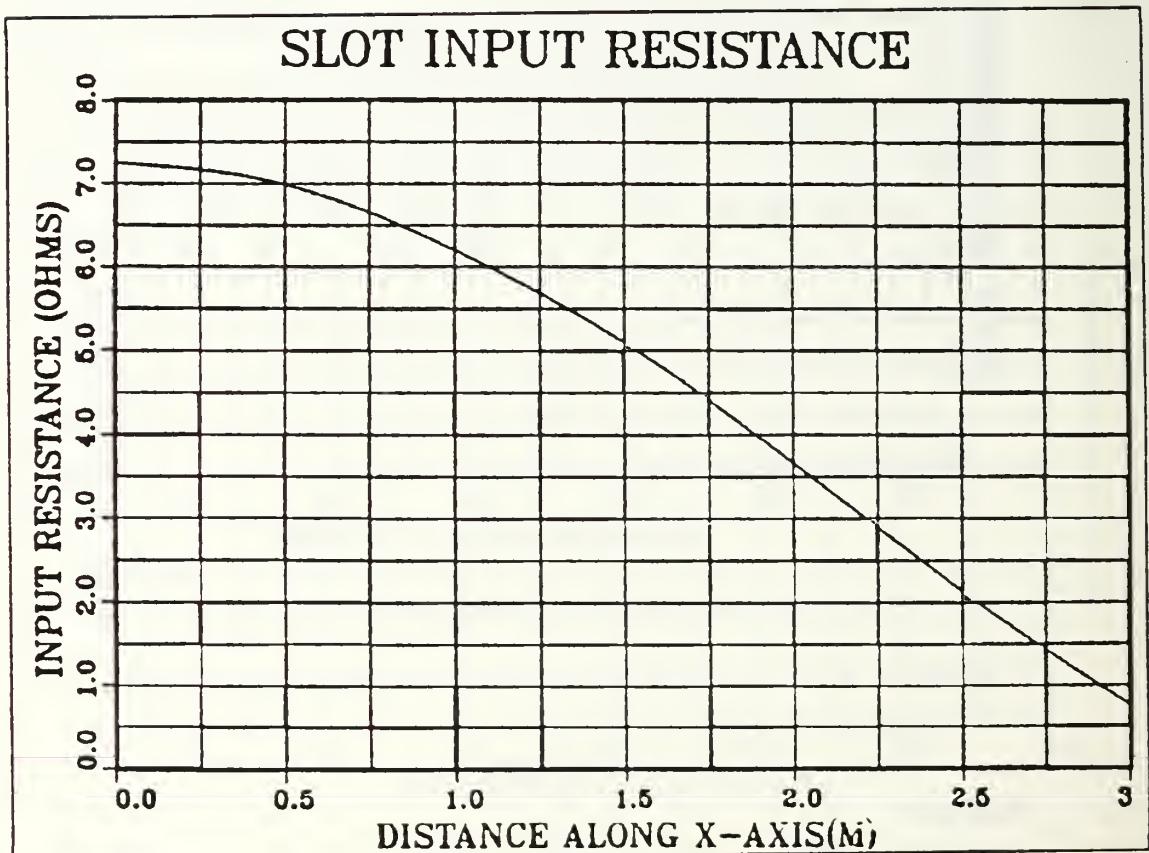
Figure C.1   Input Resistance-f=10MHz and w=0.2m.
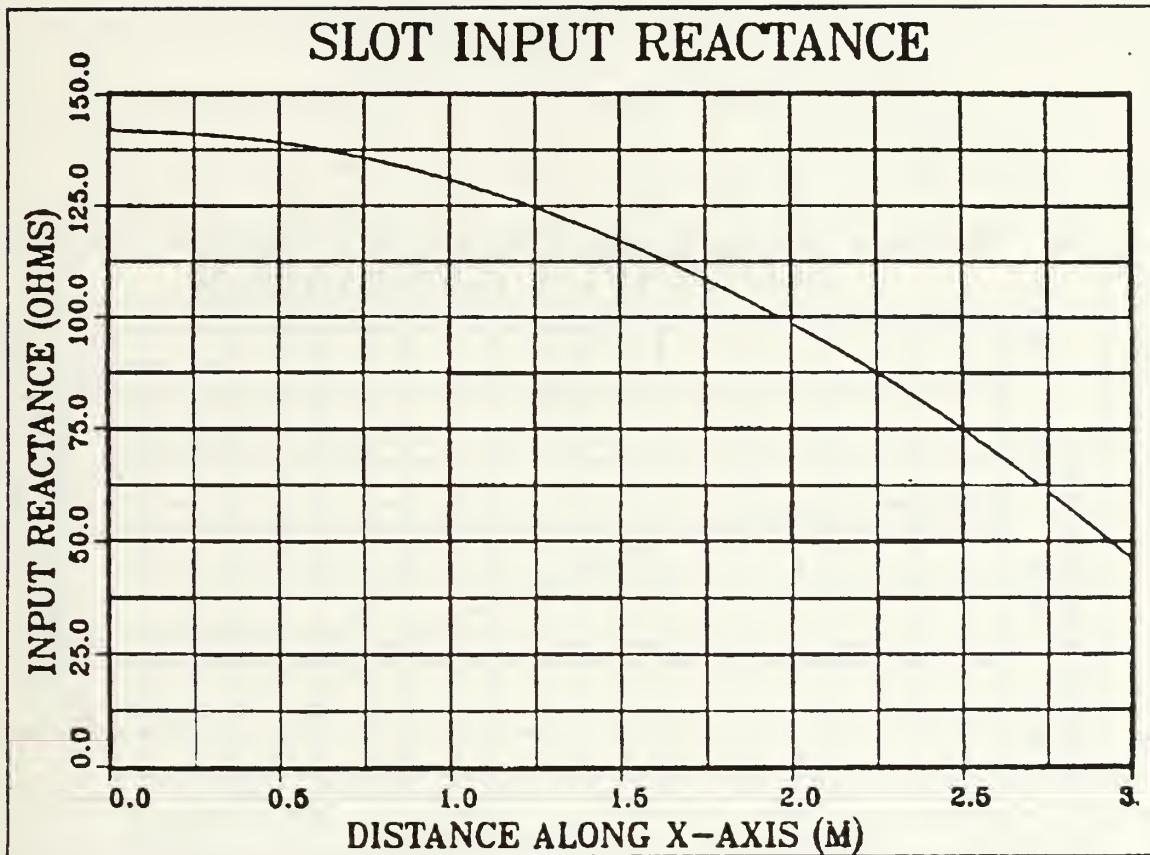
Figure C.2   Input Reactance-f=10MHz and w=0.2m.

51

SLOT INPUT IMPEDANCE FOR F=30MHZ AND W=0.2M
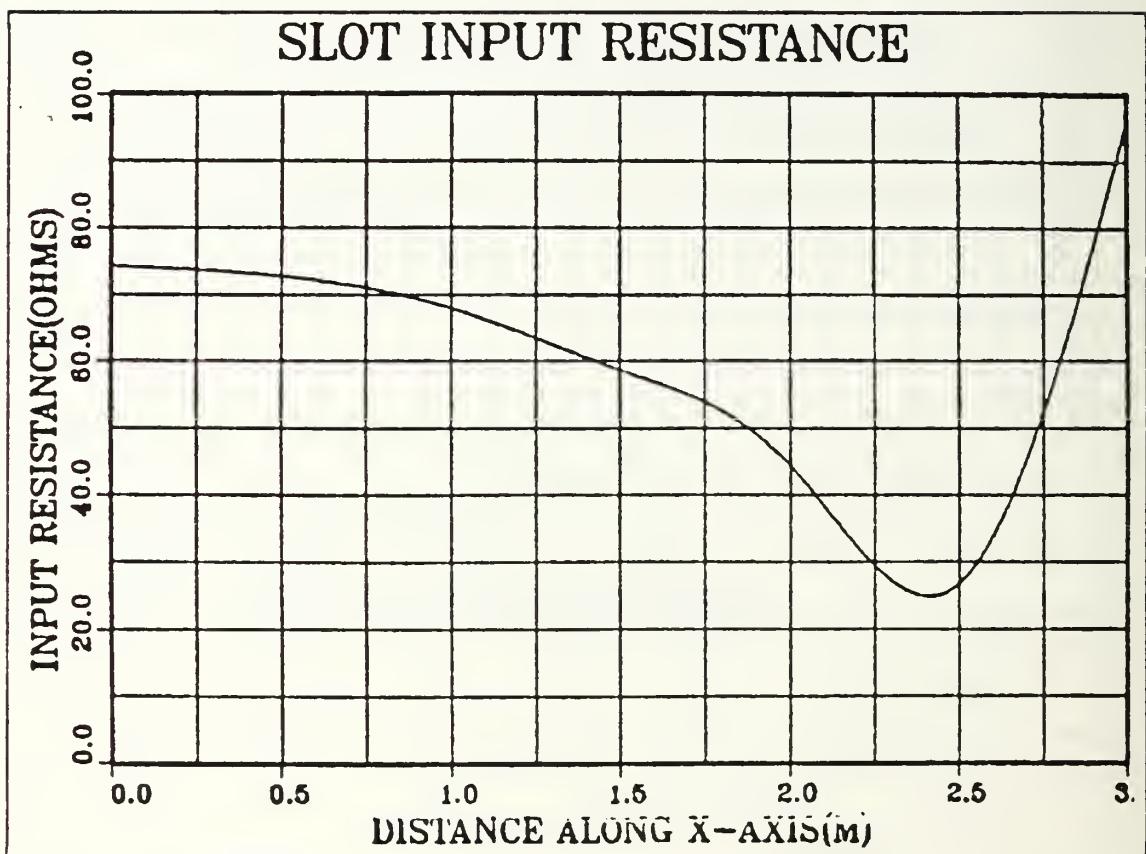
Figure D.1   Input Resistance-f=30MHZ and w=0.2m.

52
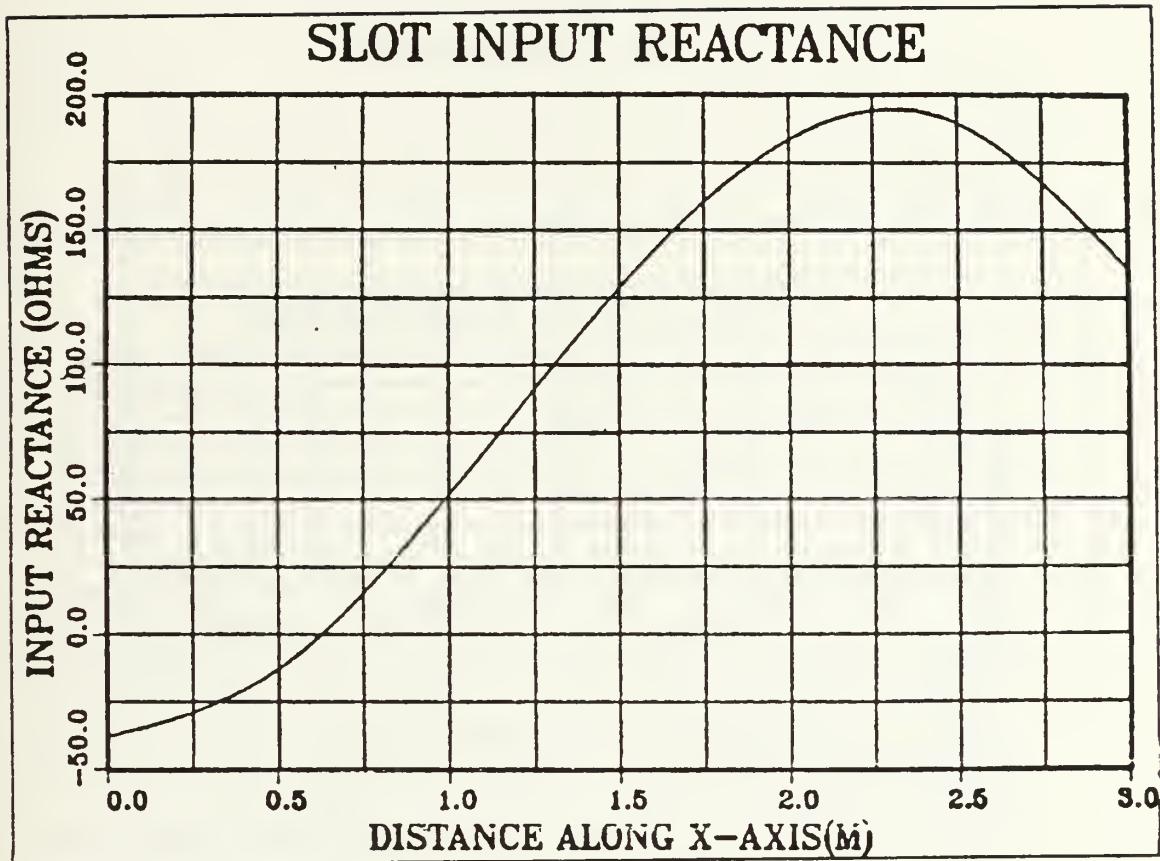
Figure D.2   Input Reactance-f=30MHz and w=0.2m.

53

SLOT INPUT IMPEDANCE FOR F=20MHZ AND W=0.5M
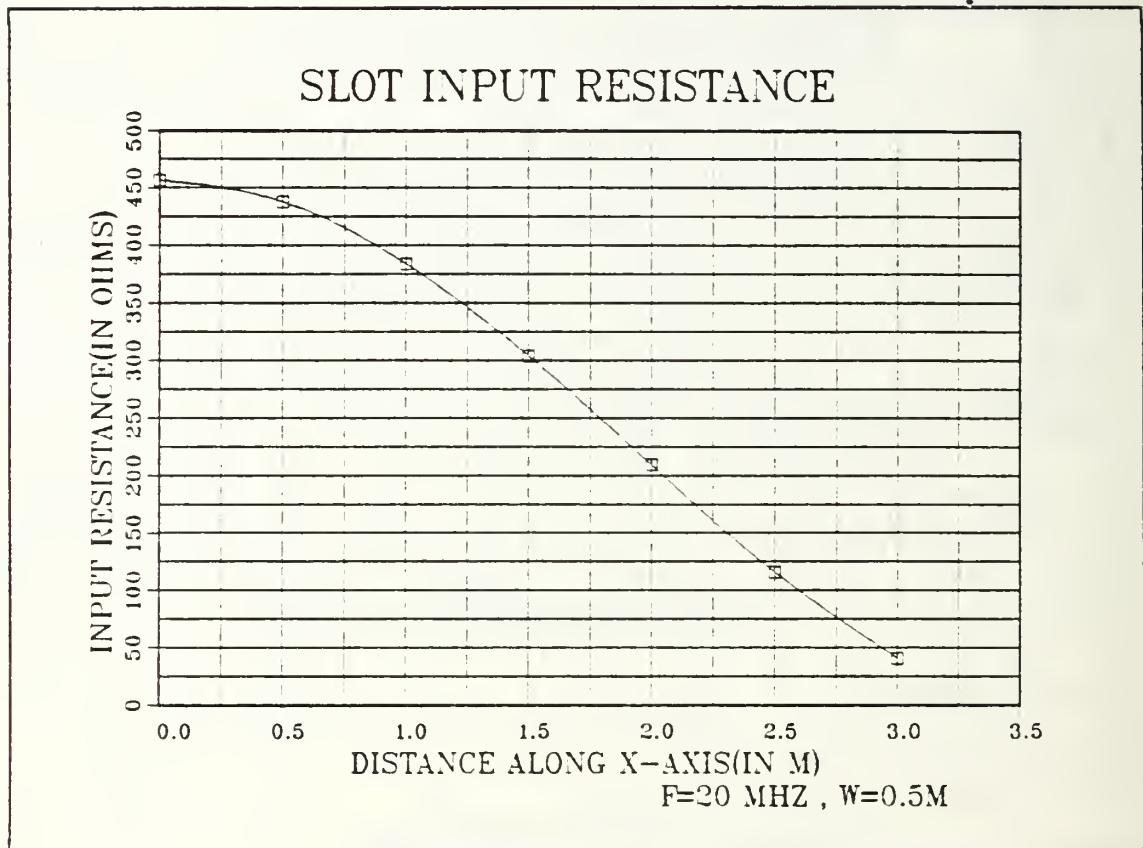


Figure E.1   Input Resistance-f=20MHz and w=0.5m.
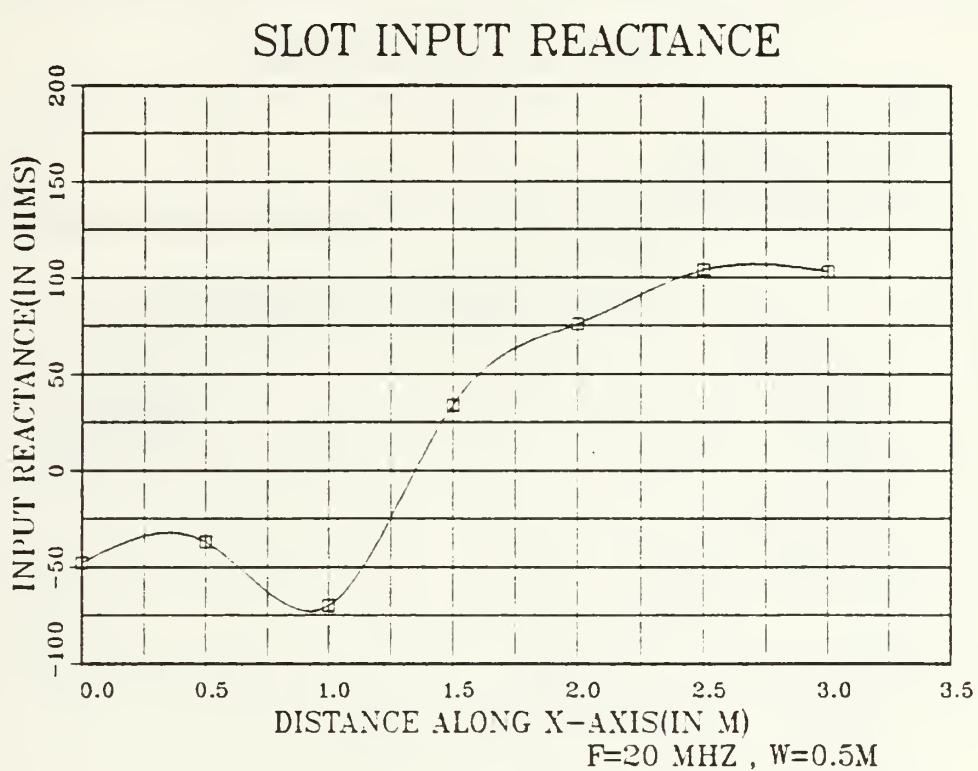
Figure E.2   Input Reactance-f=20MHz and w=0.5m.

SLOT INPUT IMPEDANCE FOR THE RANGE : 18 TO 22MHZ
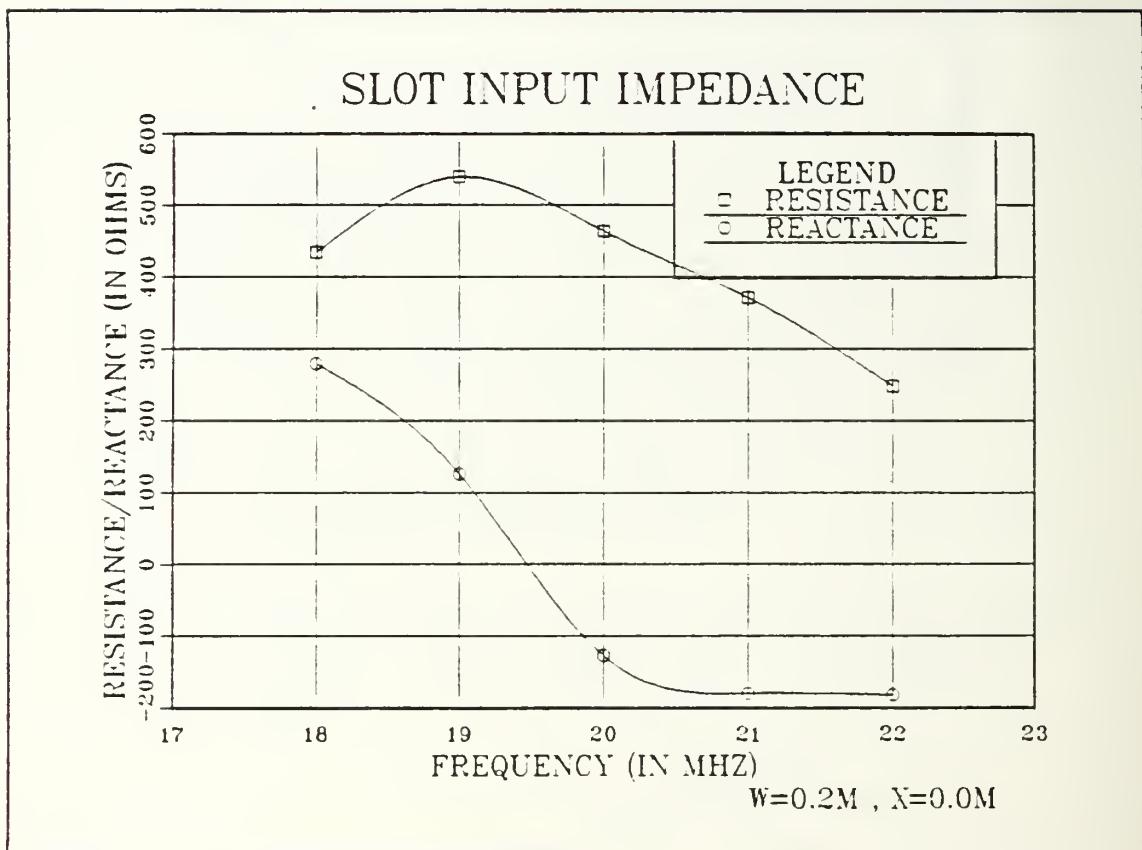

Figure F.1   Slot Input Impedance-w=0.2m and x=0.0m.
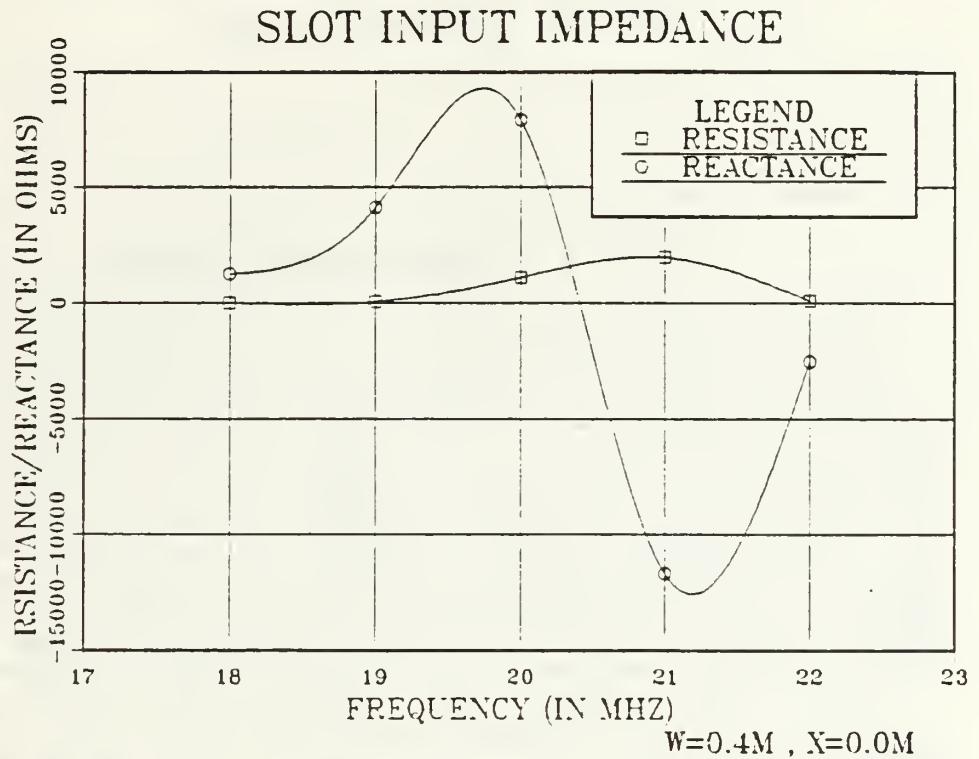
Figure F.2   Slot Input Impedance-w=0.4m and x=0.0m.

57

NEAR FIELD INSIDE THE SLOT
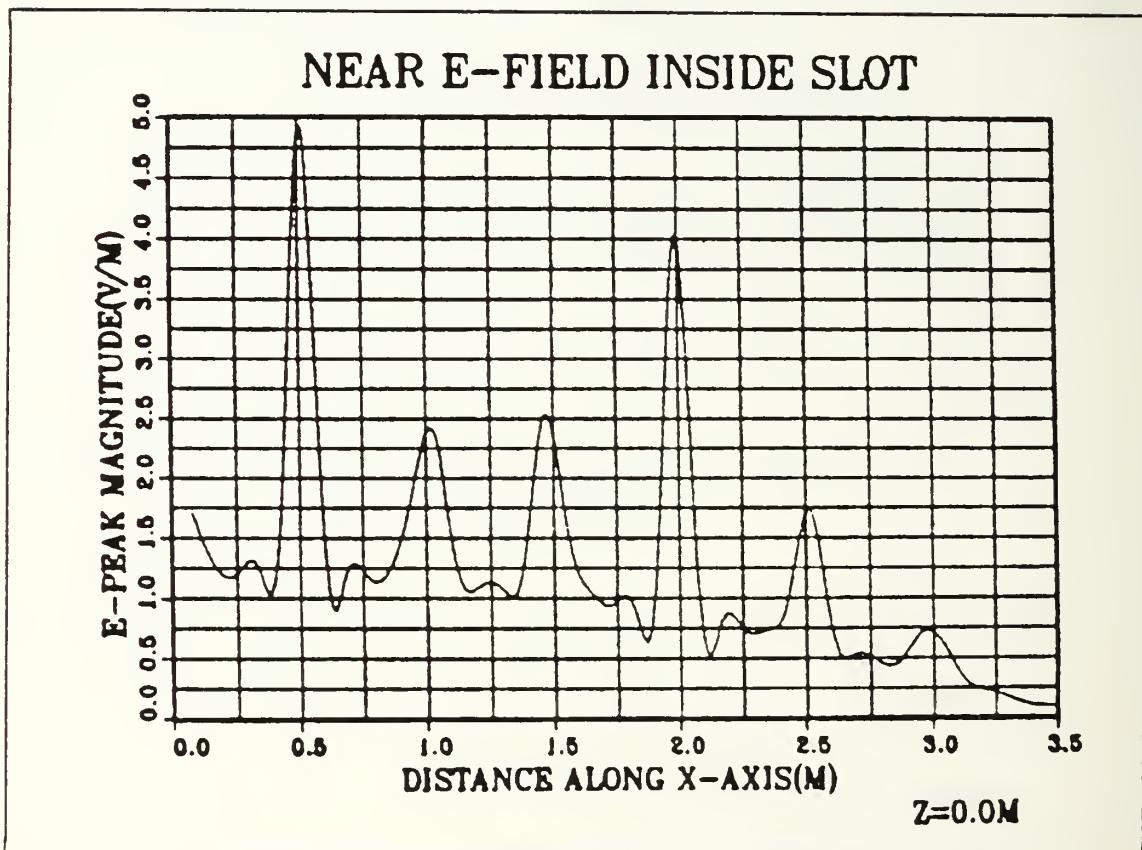
Figure G.1   Near-Field for z=0.0m.
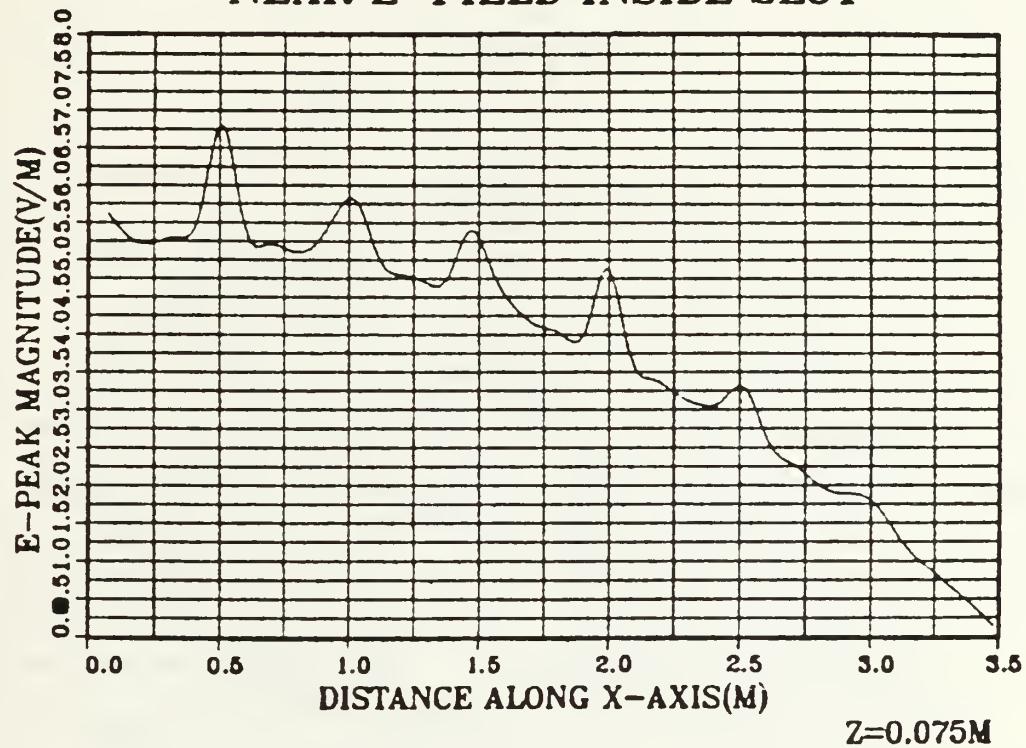
Figure G.2   Near-Field for z=0.075m.

SLOT RADIATION PATTERNS: SINGLE SOURCE
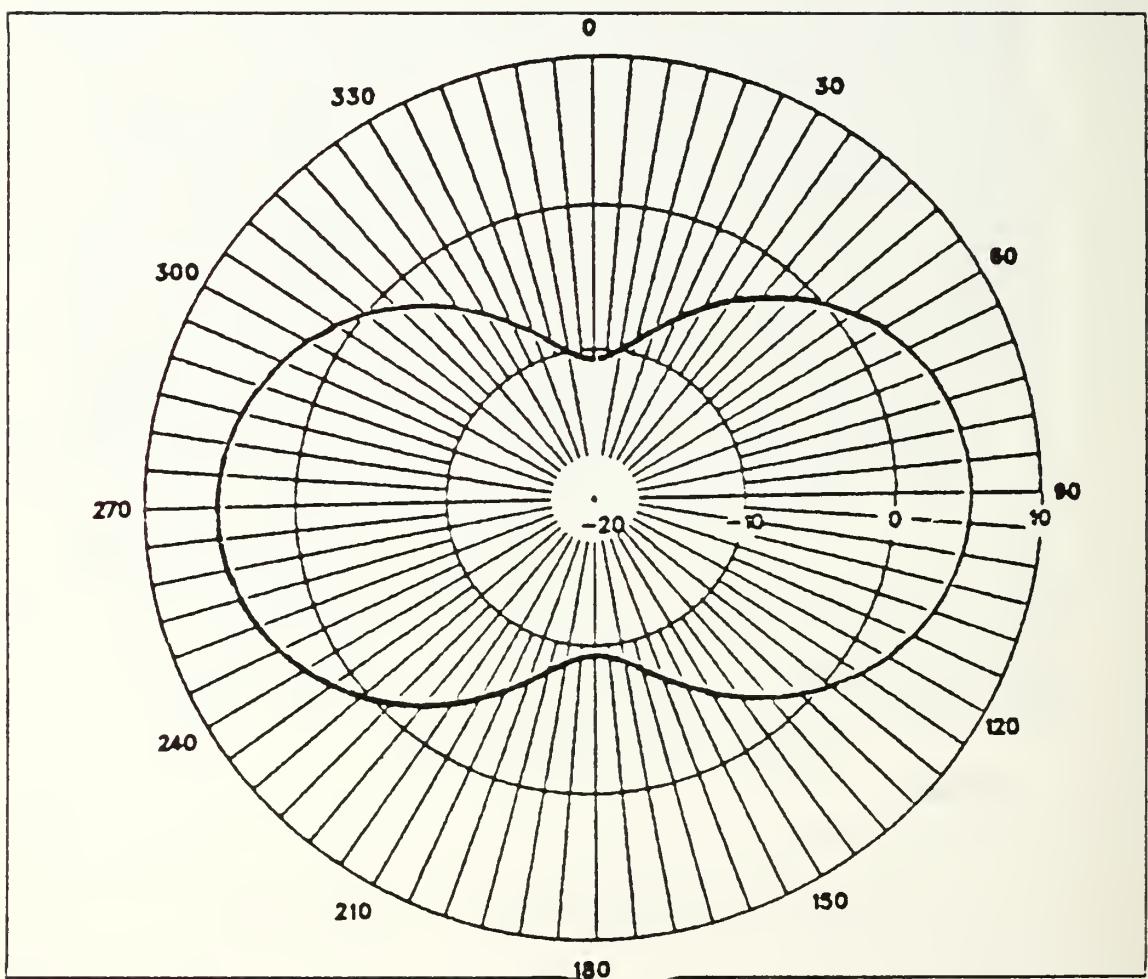
Figure H.1   E-Field Horizontal Pattern : x=0.5m.
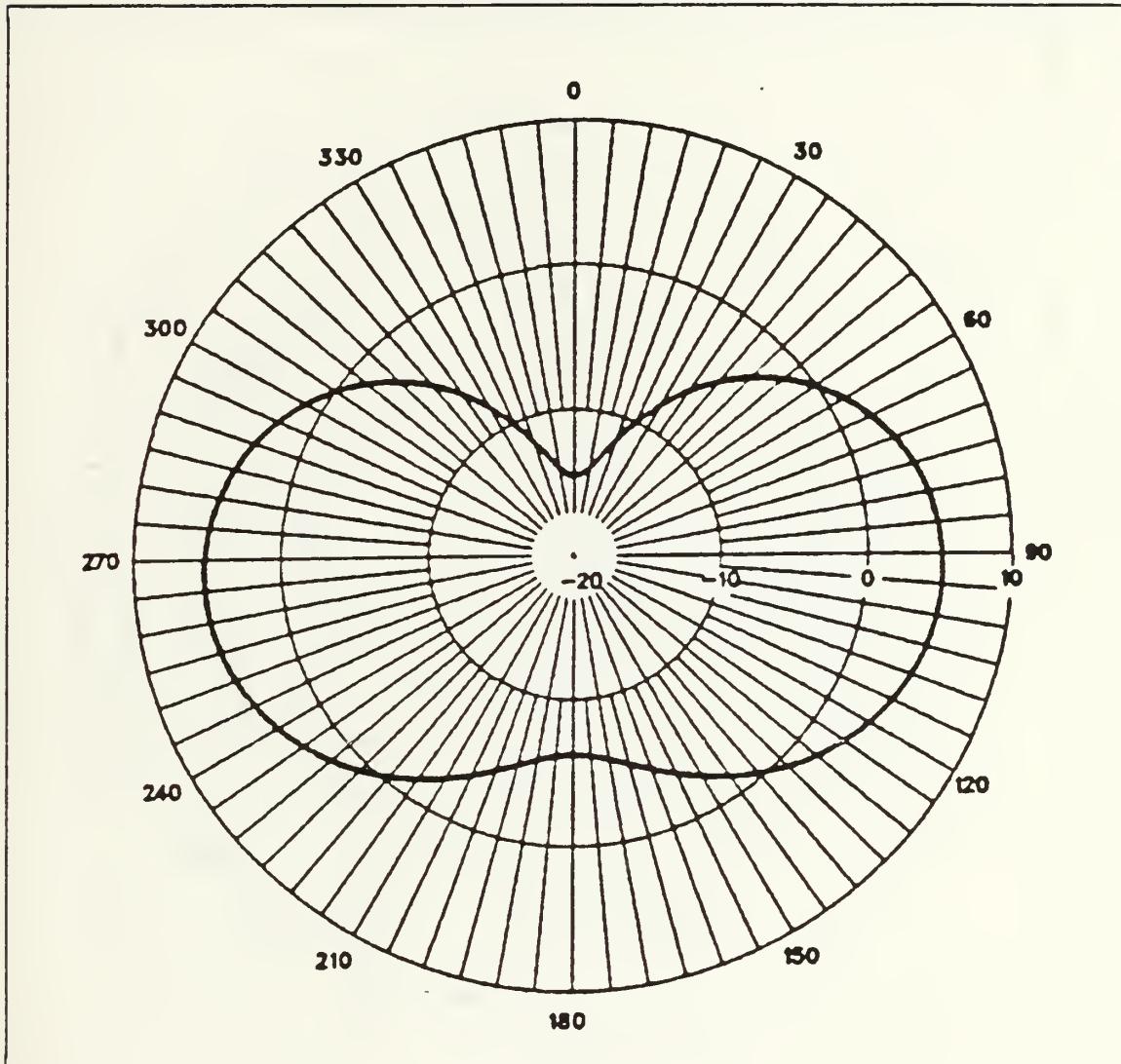
Figure H.2   E-Field Horizontal Pattern : x=3.0m.
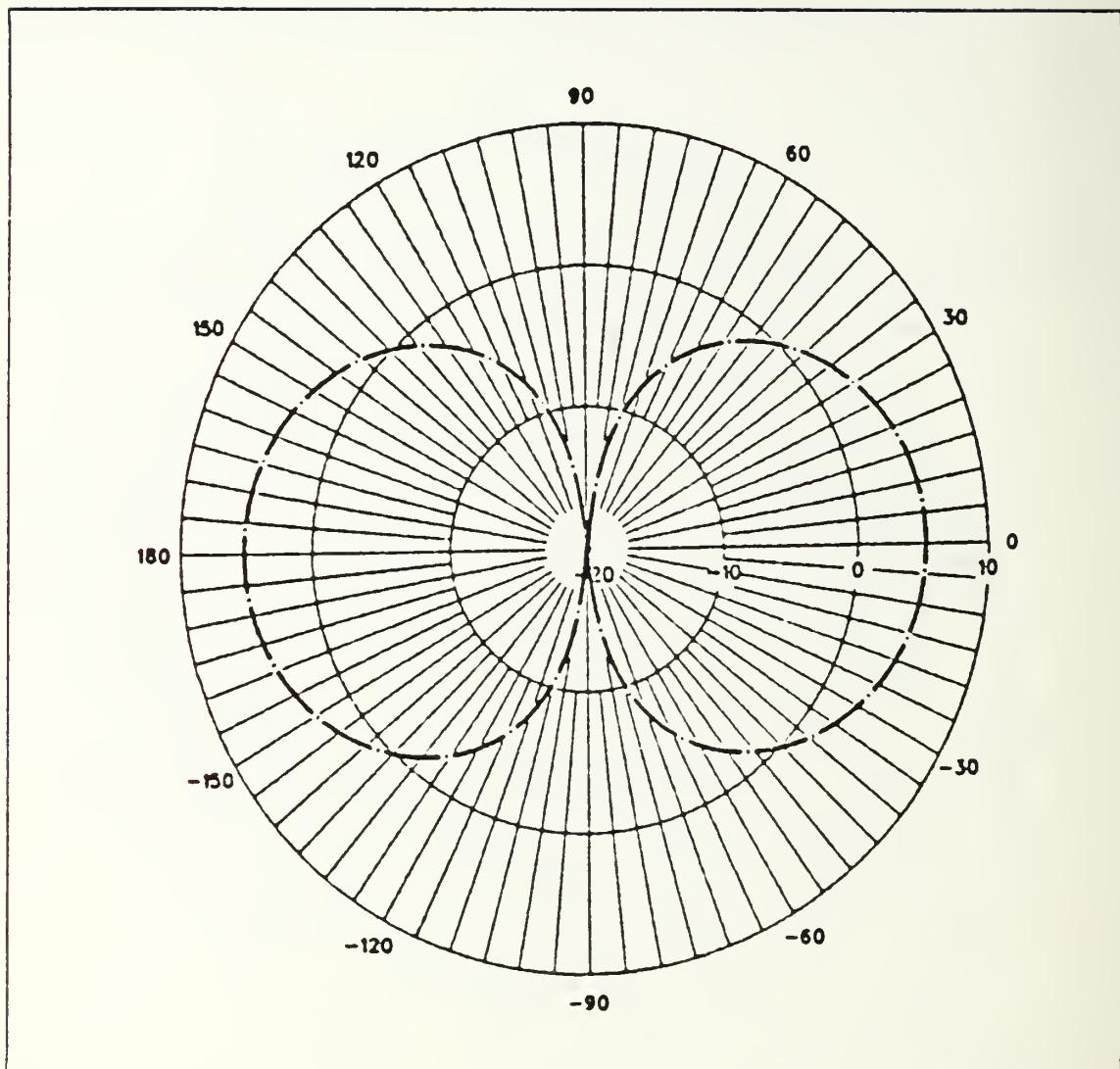
Figure H. 3   E-Field Vertical Pattern : x=0.5m.
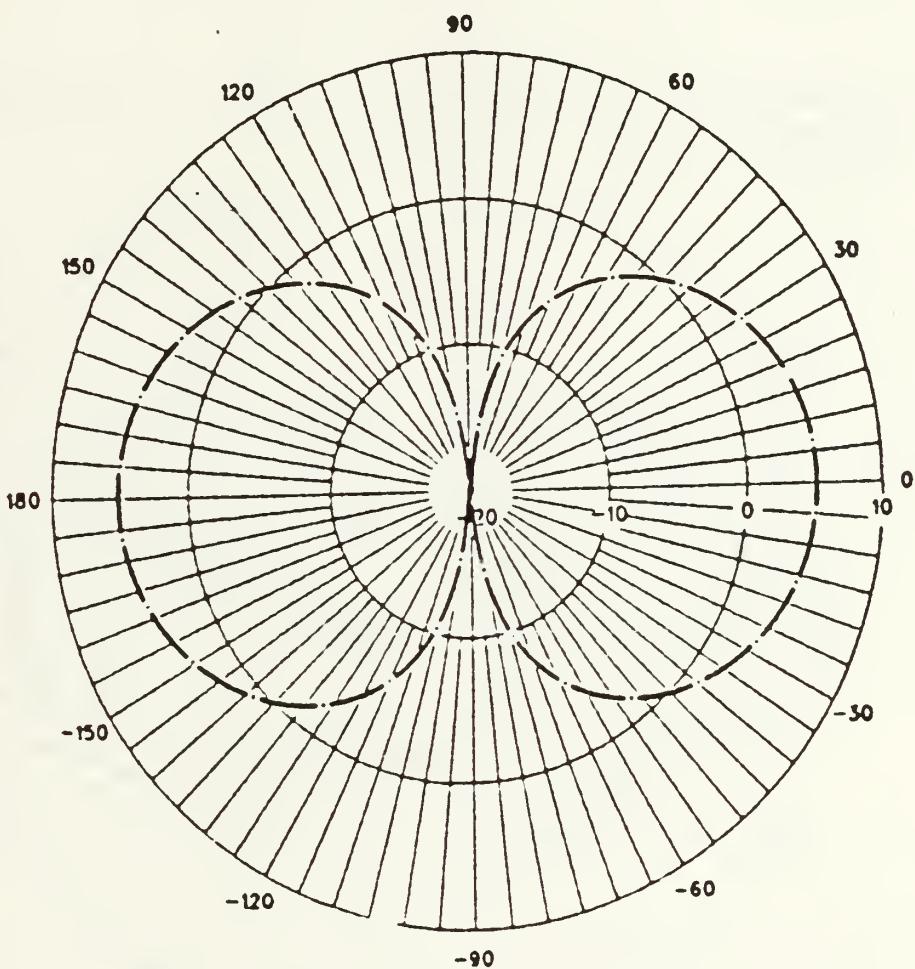
Figure H.4   E-Field Vertical Pattern : x=3.0m.

63

APPENDIX I

SLOT HORIZONTAL PATTERNS: MULTIPLE SOURCES
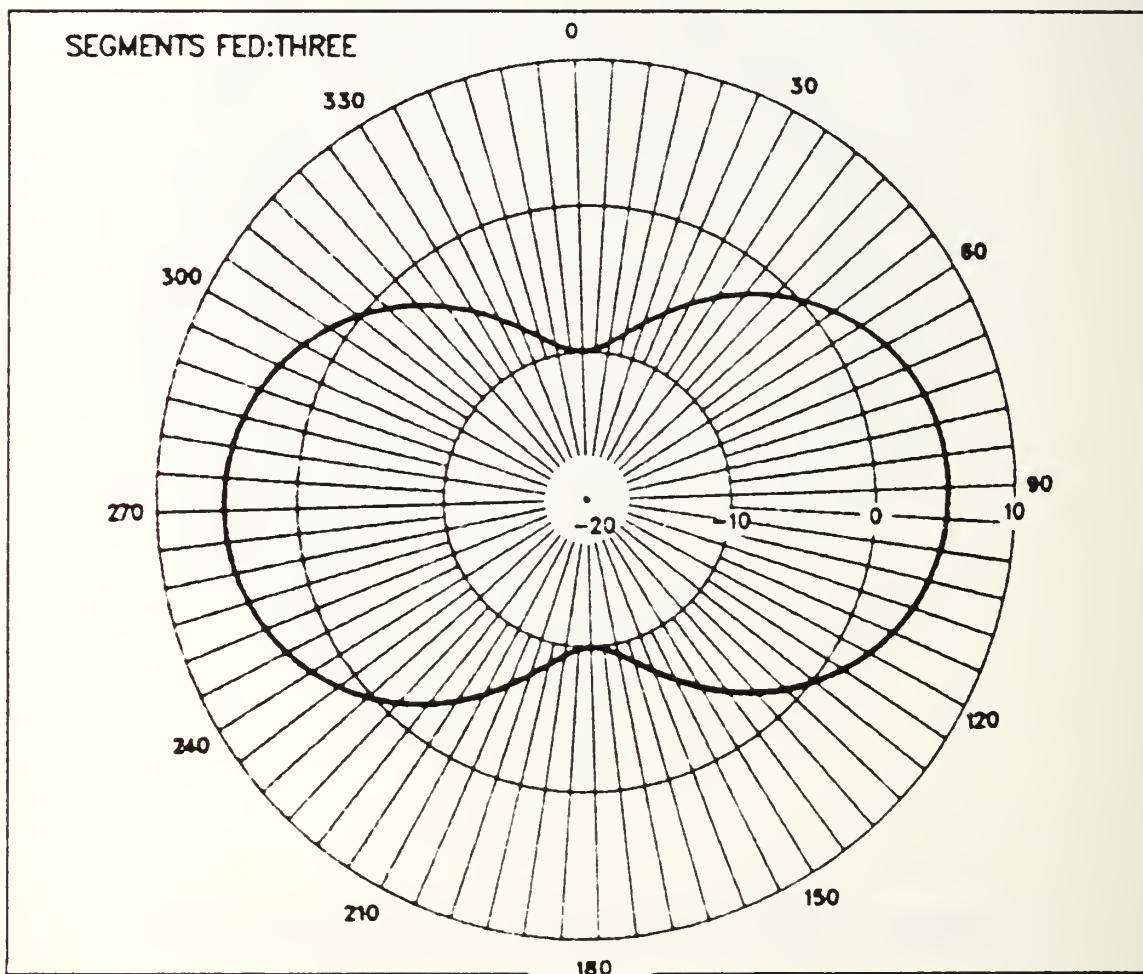
Figure I.1   E-Field Horizontal Pattern : 3 sources.

64
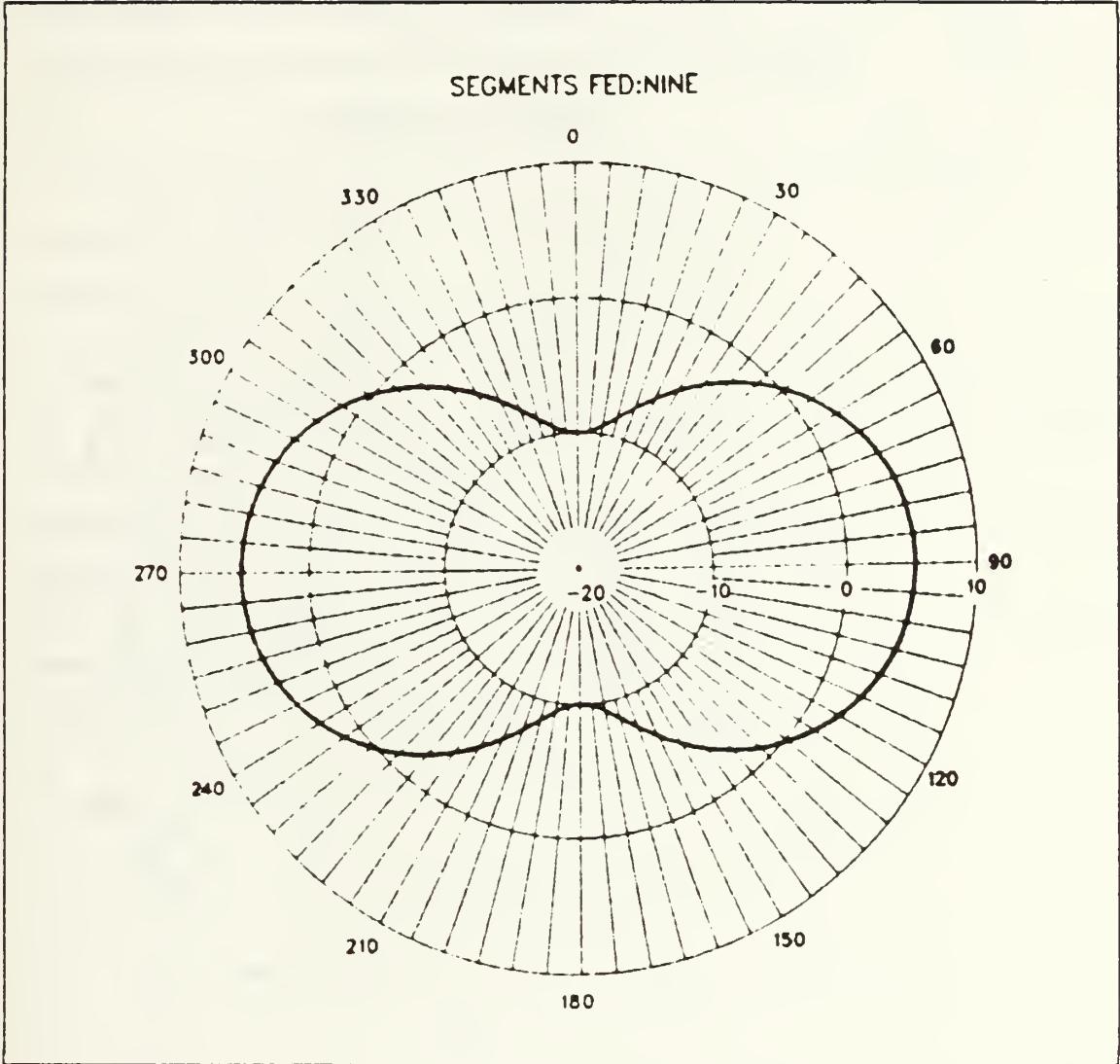
Figure I.2   E-Field Horizontal Pattern : 9 sources.

65
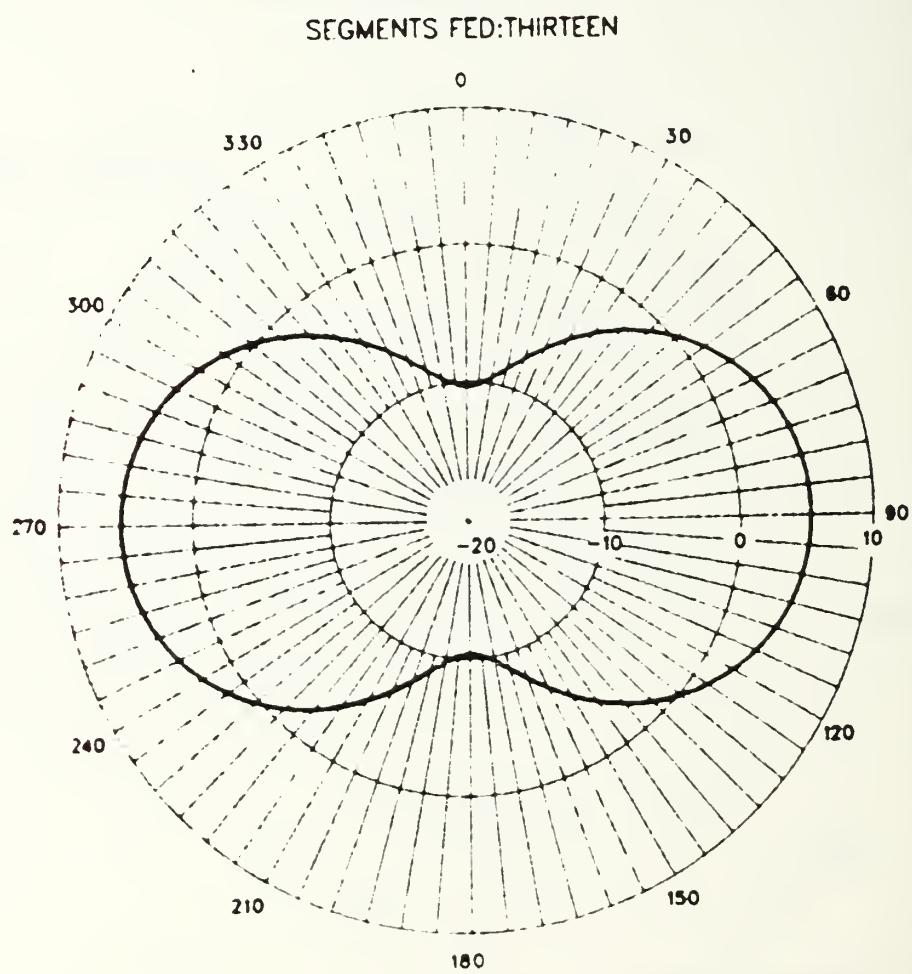
Figure I.3   E-Field Horizontal Pattern : 13 sources.

APPENDIX J

DATA SET FOR A MULTIPLY FED SLOT ANTENNA

```
//GO.SYSIN DD *
CM FEEDING THE SLOT AT THIRTEEN POINTS
CE GETTING THE NGF FOR w=0.2m and f=20.0MHz
GF
GW 600,1, 0.,0.,.100,0.,0.,-.100,.01
GW 601,1, .5,0,.100, .5,0,-.100,.01
GW 602,1, -.5,0,.100, -.5,0,-.100,.01
GW 603,1, -1.,0,.100, -1.,0,-.100,.01
GW 604,1, 1.,0,.100, 1.,0,-.100,.01
GW 605,1, 1.5,0,.100, 1.5,0,-.100,.01
GW 606,1,-1.5,0,.100,-1.5,0,-.100,.01
GW 607,1,-2.0,0,.100,-2.0,0,-.100,.01
GW 608,1, 2.0,0,.100, 2.0,0,-.100,.01
GW 609,1, 2.5,0,.100, 2.5,0,-.100,.01
GW 610,1,-2.5,0,.100,-2.5,0,-.100,.01
GW 611,1,-3.0,0,.100,-3.0,0,-.100,.01
GW 612,1, 3.0,0,.100, 3.0,0,-.100,.01
GE
EX 0,600,1
EX 0,601,1
EX 0,602,1
EX 0,603,1
EX 0,604,1
EX 0,605,1
EX 0,606,1
EX 0,607,1
EX 0,608,1
EX 0,609,1
EX 0,610,1
EX 0,611,1
```

67

```
EX 0,612,1
PL 3,2,0,4
RP 0,1,361,1000,90,0,0,1
EN
//*
//*
/*
```

LIST OF REFERENCES

1. Young, A., _An Application of Approximate Product-Integration to the Numerical Solution of Integral Equations_, Proc. of Royal Soc.,London, Set A, 224, No.3, pp.552-573,1954.

2. Mei, K. K., _On the Integral Equation of Thin Wire Antennas_, IEEE Transactions on Antennas and Propagation, Vol. 13, pp. 374-378,May 1965.

3. Harrington, R. F., _Matrix Methods for Field Problems_, Proceedings of IEEE, Vol. 55, pp. 136-149,February 1967.

4. Begovitch, N., _Slot Antennas_, Proceeding of IRE, Vol. 38, pp. 803-806,July 1950.

5. Burke, G. J. and others, _Numerical Electromagnetics Code-A Program for Antenna System Analysis_, Lawrence Livermore Laboratory, December 1978.

6. Miller, E. K., _Wires and Wiregrid Models for Radiation and Scattering Including Grounding Effects_, Lawrence Livermore Laboratory, May 1979.

7. Burke , M. S. and Pogio, A. J., _Numerical Electromagnetics Code (NEC)- Method of Moments_, Lawrence Livermore Laboratory, January 1981.

8. Kraus , J. D., _Antennas_, McGraw-Hill, Chapter 13, 1950.

9. Booker, H. G., _Slot Aerials and their Relation to Complementary Wire Antennas_, Journal of the IEE , London, Vol.93, Part IIIA, No. 4, 1946.

10. Thomson, D.D., _Electromagnetic Near-Field Computations for a Broadcasting Monopole Using NEC_, NPS, Chap. III, September 1983

11. Harrington, R.F., _Field Computation by Moment Methods_, The Mcmillan Company of New York, Chapter 1, 1964.

12. Adler, R.W., Aperture Antennas Class Notes, NPS, 1985.

13. Funke, J.L., _Wire-Grid Modeling of Slot Antennas_, Applied Computational Electromagnetics Newsletter, Vol.1,No.1, February 1986.

BIBLIOGRAPHY

Evans,G.R., <u>Slot Antenna Studies:An Annotated Bibliography</u>, Lockheed,Missiles and Space Company,1963.

Jasik, H. and Johnson, R.C., <u>Antenna Engineering Handbook</u>, McGraw-Hill, 1984.

Jordan,E.C. and Balmain,K.G., <u>Electromagnetic Waves and Radiating Systems</u>, Prentice-Hall,1968.

Ramo,S. and others, <u>Field and Waves in Communications Electronics</u>, Wiley,1965.

<u>Reference Data for Radio Engineers</u>, ITT,1963.

Shen,L.C. and Kong,J.A., <u>Applied Electromagnetism</u>, Brooks/Cole Engineering Division,1983.

Skilling,H.H., <u>Fundamentals of Electric Waves</u>, Krieger,1974.

Stutzman, W.L. and Thiele, G. A., <u>Antenna Theory and Design</u>, Wiley, 1981.

<u>Webster's New Collegiate Dictionary</u>, Merriam-Webster,1974.

INITIAL DISTRIBUTION LIST

		No. Copies
1.	Defense Technical Information Center Cameron Station Alexandria, Virginia 22304-6145	2
2.	Library, Code 0142 Naval Postgraduate School Monterey, CA., 93943-5000	2
3.	Prof. Harriet B. Rigas,Code 62Rr Chairman of Department of Electrical Engineering Naval Postgraduate School Monterey, CA. 93943-5000	1
4.	Dr. Richard W. Adler, Code 62Ab Naval Postgraduate School Monterey, CA., 93943-5000	5
5.	Prof. Hung-Mou Lee,Code 62Lh Naval Postgraduate School Monterey, CA., 93943-5000	1
6.	Mario C. Neiva Brazilian Naval Commission 4706 Wisconsin Ave., N.W. Washington, DC, 20016	2
7.	Lt. J.C. Tertocha C/o Tina Boggs 6711 Agnes St. N.Hollywood, CA.91606	1
8.	Dr. Stephen Jaurequi, Code 62Ja Naval Postgraduate School Monterey, CA., 93943-5000	1
9.	W.F. Flanigan, Code 825 Naval Ocean Systems Center 271 Catalina Blvd. San Diego, California 92152	1
10.	D. Washburn, Code 7403 Naval Ocean Systems Center 271 Catalina Blvd. San Diego, California 92152	1
11.	Jim Logan, Code 822 Naval Ocean Systems Center 271 Catalina Blvd. San Diego, California 92152	1
12.	Rick Thowless, Code 822 Naval Ocean Systems Center 271 Catalina Blvd. San Diego, California 92152	1
13.	M. Selkellick, Code 1202 David Taylor Naval Ship Research Development Center Betheseda, Maryland 20084-5000	1

14. Jim K. Breakall   1
    Lawrence Livermore National Laboratory
    P.O.Box 5504, 1-156
    Livermore, CA. 94550

15. G. Burke   1
    Lawrence Livermore National Laboratory
    P.O.Box 5504, 1-156
    Livermore, CA. 94550

16. E. Domning   1
    Lawrence Livermore National Laboratory
    P.O.Box 5504, 1-156
    Livermore, CA. 94550

17. Robert Latorre   1
    Lawrence Livermore National Laboratory
    P.O.Box 5504, 1-156
    Livermore, CA. 94550

18. Donn Cambell   1
    CECOM-CENCOMS
    Fort Monmouth, New Jersey 07703

19. Ron Corry   1
    USAISEA/ASBH-SET-P
    Fort Huachuca, Arizona 85613-5300

20. Bill Alvarez   1
    USAISEA/ASBH-SET-P
    Fort Huachuca, Arizona 85613-5300

21. Janet McDonald   1
    USAISEA/ASBH-SET-P
    Fort Huachuca, Arizona 85613-5300

22. Dr. Tom Tice   1
    Dept. of Electrical and Computer Enginnering
    Arizona State University
    Tempe, Arizona 85287

23. Dr. Roger C. Rudduck   1
    Electrophysics Laboratory
    Ohio State University
    1320 Kinnear Rd.
    Colombus, Ohio 43212

24. Commander Naval Space and Naval Warfare   1
       Systems Command
    Attention:Dick Pride
    PDW 110-243
    Washigton D.C. 20363

25. Naval Sea Systems Command   1
    Attention:P. Law
    C61X41
    Washigton D.C. 20362

26. Costas Theofanopoulos   1
    355 Casa Verde Way #8
    Monterey, CA., 93940

27. Ioannis Vorrias   1
    1001 Funston Ave. #3
    Monterey, CA., 93940

28. George Lymberopoulos   1
    1001 Funston Ave. #3
    Monterey, CA., 93940

29. Director Research Administration, Code 012   1
    Naval Postgraduate School
    Monterey, CA., 93943-5000